

Physiologically Based Pharmacokinetic Modelling
EPA Scientific Advisory Panel
24 - 27 October 2017

Syngenta White Paper

- 1. Proof of Concept Study That Addresses the Lack of Human *In Vivo* Data in the Agrochemical Regulatory Environment by Employing a Population Based IVIVE-PBPK Modelling & Simulation Approach to Predict Human Internal Dosimetry**
- 2. Demonstration of Derivation of Data Derived Extrapolation Factors to Reduce Uncertainty in Human Health Risk Assessments**
- 3. Representation of the Relative Internal Dosimetry Between Consumers and the Human Equivalent Dose as Indicated by a Toxicologically Determined Point of Departure Indicating a ‘Toxicokinetic Safety Margin’**

Table of Contents

Table of Contents	2
Abbreviations	5
1 PBPK Scientific Advisory Panel Syngenta Submission Documents	7
1.1 Syngenta White Paper	8
1.2 PBPK Modelling and Simulation Report	8
1.3 Supporting Documentation – Relevant Simcyp & White Paper References.....	8
1.4 Supporting Documentation – Simcyp Input and Output Files	8
1.5 Supporting Documentation – <i>In Vitro</i> and <i>In Vivo</i> Study Reports	9
2 Executive Summary	9
3 Introduction.....	10
4 The Simcyp Population Based Simulator Platform	13
4.1 General Background	13
4.2 Simcyp Version and Base PBPK Model	14
4.3 Building Virtual Individuals	16
5 IVIVE-PBPK Proof of Concept Objectives.....	17
6 Acibenzolar	18
6.1 Synonyms	18
6.2 Toxicity Endpoint & Point of Departure	19
6.2.1 Toxicity Endpoint	19
6.2.2 Point of Departure for Risk Assessment Purposes	19
6.3 Rat <i>In Vivo</i> Absorption, Distribution, Metabolism and Excretion	19
7 IVIVE-PBPK Modelling and Simulation Approach	19
8 Acibenzolar <i>In Vitro</i> ADME Studies (Rat & Human).....	21
8.1 <i>In Vitro</i> Investigations Carried Out	21
8.2 Free Fraction in Plasma & Blood to Plasma Ratios	21
8.3 <i>In Vitro</i> Metabolism.....	21
9 Acibenzolar <i>In Vivo</i> Studies in Rat.....	23
9.1 <i>In Vivo</i> Toxicokinetic Study Design.....	23
9.2 <i>In Vivo</i> Toxicokinetic Study Results	24
9.2.1 Intravenous Dose Toxicokinetics (1 mg/kg).....	25
9.2.2 Oral Dose Toxicokinetics (1, 10 and 100 mg/kg).....	25
10 Consumer Exposure to Acibenzolar via Food and Drinking Water	26

11	Identification of Potentially ‘At Risk’ Populations	27
12	Doses for Simulation of Acute and Chronic Exposure Scenarios	27
13	Development, Verification and Output of Rat and Human PBPK Modelling and Simulation	28
13.1	Rat PBPK Model	28
13.1.1	Distribution and blood binding	28
13.1.2	Absorption.....	29
13.1.3	Elimination.....	29
13.1.4	Rat PBPK Model Input Parameters	30
13.1.5	Incorporating Variability into Rat PBPK Model	31
13.1.6	Understanding Variability – Rat PBPK Model Sensitivity Analysis.....	32
13.1.7	PBPK Model Acceptance	33
13.1.8	Simulation of Dietary Administration and POD Study	34
13.2	Human PBPK Model	37
13.2.1	Distribution and Blood Binding.....	37
13.2.2	Absorption.....	38
13.2.3	Elimination.....	38
13.2.4	Human PBPK Model Input Parameters	40
13.2.5	Human PBPK Model Sensitivity Analysis	41
13.3	Dose Proportionality, Human Equivalent Dose Derivation and Simulation of Internal Dosimetry at the POD	42
13.3.1	Dose Proportionality	42
13.3.2	Human Equivalent Dose	42
13.3.3	Simulation of Human Internal Dosimetry at the HED.....	43
13.4	Simcyp Human Population Libraries and Simulation Scenarios.....	43
13.5	Simulations of Consumer Exposure Scenarios in Adults, Children (1 – 2 years) and Renally Impaired Populations.....	44
14	Application of Population based PBPK Models to Obtain Toxicokinetic Data Derived Extrapolation Factors and Toxicokinetic Composite Factors.....	48
14.1	Toxicokinetic Data Derived Extrapolation Factors EF_{AK} & EF_{HK}	48
14.1.1	Selection of Dose Metric	48
14.1.2	Human Equivalent Dose and Animal to Human Interspecies Toxicokinetic Extrapolation Factor, EF_{AK}	48
14.1.3	Defining Interindividual Variability in Human Populations - Intraspecies Toxicokinetic Extrapolation Factor, EF_{HK}	49
14.2	Toxicokinetic Composite Factors	50

15	Composite Factors for Risk Assessment	50
16	Acibenzolar Example Risk Assessment Employing Toxicokinetic DDEFs	51
17	Application of Human PBPK Model to Indicate Toxicokinetic Safety Margins	52
18	Conclusion	54
19	References.....	55
	Appendix 1: Toxicology Endpoints and Point of Departure	59
	Appendix 2: PBPK Model Input, Output and R Script Files Provided to the SAP	61

Abbreviations

ADME	Absorption, Distribution, Metabolism and Excretion
AD _{UF}	Uncertainty factor for animal to human differences in toxicodynamics
AK _{UF}	Uncertainty factor for animal to human differences in toxicokinetics
AUC	Area under the curve
AUC _{last}	Area under the curve to the last measured (simulated) time point
AUC _{inf}	Area under the curve extrapolated to infinity
AUC _{extrapolated}	The percentage of AUC to infinity estimated by extrapolation of the terminal phase.
AUC _{312,336}	Area under the curve on day 14 of dosing (312 to 336 hours post first dose)
AUC _{0,24}	Area under the curve from 0 to 24 hours post first dose
BCRP	Breast cancer resistance protein
B/P	Blood to plasma ratio
BW	Body weight
Caco-2	Human epithelial colorectal adenocarcinoma cells
CES	Carboxylesterase
CF	Composite factor
CF _{TK}	Toxicokinetic composite factor
C _{max}	Maximum concentration
CL	Clearance
CL/F	Apparent clearance following oral dosing
CL _{int}	Intrinsic clearance
CL _{u,int-H}	Scaled unbound intrinsic clearance of compound in the liver
CL _r	Renal clearance
C _p	Systemic concentration of compound in plasma
C _{pv}	Concentration of compound in the portal vein blood
C _{Liv}	Total concentration of compound in the liver
C _{u,Liv}	Unbound concentration of compound in the liver
CV	Coefficient of variation
DDEF	Data derived extrapolation factor
DNT	Developmental Neurotoxicity
e	Erythrocyte
EDWC	Estimated drinking water concentration
EF _{AD}	Interspecies toxicodynamic extrapolation factor
EF _{AK}	Interspecies toxicokinetic extrapolation factor
EF _{HD}	Intraspecies toxicodynamic extrapolation factor
EF _{HK}	Intraspecies toxicokinetic extrapolation factor
E/P	Erythrocyte:plasma ratio
fa	Fraction absorbed
fe	Fraction excreted
F _G	Availability of compound escaping first pass metabolism in the intestine
fu	Fraction unbound in plasma
fu _{gut}	Fraction unbound in the portal vein
fu _{inc}	Fraction unbound in an incubation (non-specific binding)

GFR	Glomerular Filtration Rate
h	Hour
HD _{UF}	Uncertainty factor for human variability in toxicodynamics
HK _{UF}	Uncertainty factor for human variability in toxicokinetics
HED	Human Equivalent Dose
HPGL	Hepatocytes per gram of liver
IV	Intravenous
IVIVE	<i>In vitro</i> to <i>in vivo</i> extrapolation
K _a	First order absorption rate constant
K _m	Michaelis constant
K _p	Liver to plasma partition coefficient
LW	Liver weight
MPPGL	Microsomal protein per gram of liver
p	Plasma
PBPK	Physiologically based pharmacokinetic
PD	Pharmacodynamics
P-gp	p-glycoprotein
PK	Pharmacokinetic
PMRA	Pest management regulatory agency
PO	Oral
POD	Point of departure
Q _{HA}	Blood flow in the hepatic artery
Q _{Liv}	Total hepatic blood flow
Q _{PV}	Blood flow in the hepatic portal vein
QSAR	Quantitative Structure Activity Relationship
SD	Standard deviation
t	Tissue
t _{1/2}	Half life
TD	Toxicodynamic
TD _{UF}	Toxicodynamic uncertainty factor
TK	Toxicokinetic
t _{max}	Time at which maximum concentration occurs
TSM	Toxicokinetic safety margin
US EPA	US Environmental Protection Agency
V	Fractional body volume
V _{Liv}	Volume of liver
V _{max}	Maximum rate of metabolism
V _{ss}	Volume of distribution at steady state
WHO	World health Organization

1 PBPK Scientific Advisory Panel Syngenta Submission Documents

As part of the EPA PBPK SAP Syngenta sets out a ‘proof of concept’ study to demonstrate how a population based *in vitro* to *in vivo* extrapolation (IVIVE)-physiologically based pharmacokinetic (PBPK) modelling and simulation approach can predict internal dosimetry within human populations and the outputs implemented into reducing uncertainty in human health risk assessments.

The approach outlined in this white paper addresses toxicokinetic uncertainty only; toxicodynamic uncertainty is not addressed.

Specifically for this study, a model compound (Acibenzolar-S-Methyl) and the Simcyp population based simulator platform are used. Although not essential to assess the merits of the approach employed access to the Simcyp simulator platform software can be provided to SAP panel members if requested.

The submission comprises of a White Paper providing an overview and example risk assessments, a separate detailed account of the modelling and simulations employed using the Simcyp simulator platform and supporting documentation as outlined in figure 1 and followed by a brief description below. A more detailed listing of the supporting documentation (including a breakdown of file names and content) is also provided in appendix 2.

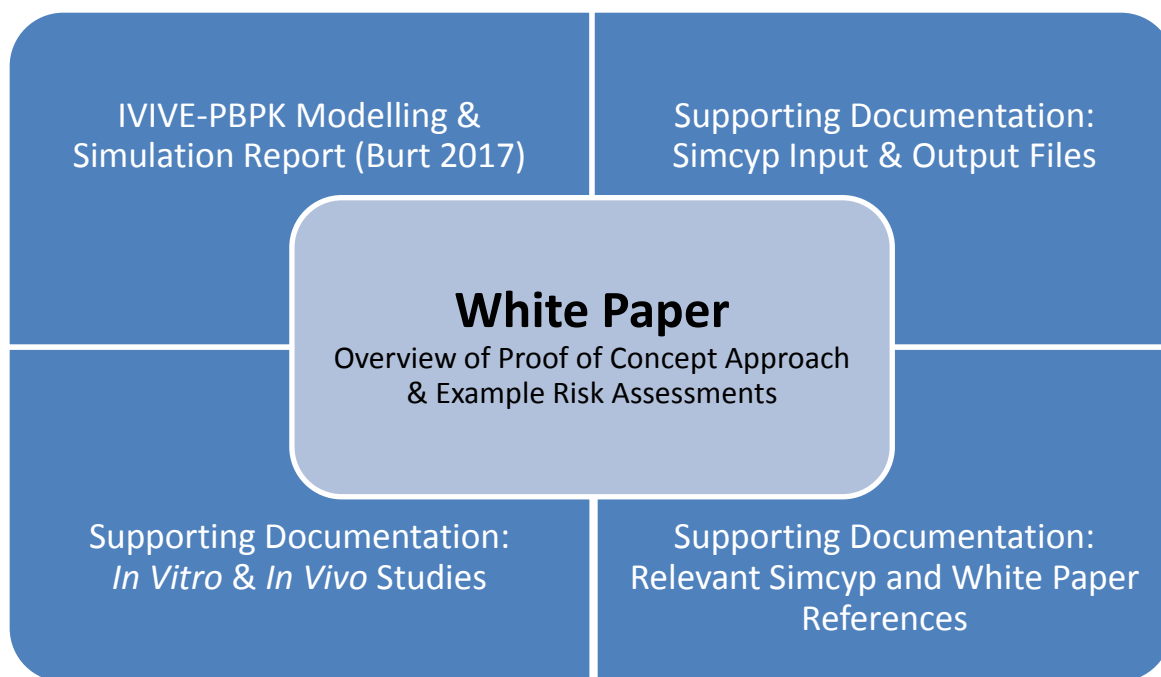


Figure 1: Outline of Syngenta submission to the EPA PBPK SAP including a White Paper to provide an overview of the overall approach and a guide to further more detailed information contained in supporting documentation.

1.1 Syngenta White Paper

This White Paper provides details of the population based IVIVE-PBPK approach employed together with an overview of the rat and human model development and verification including summaries of the model inputs and outputs and example human health risk assessments utilizing the data obtained. This report should be read first.

Background is also provided on the Simcyp population based simulator platform including information on the Simcyp platform history and construction, references to key algorithms used in the software, how individuals are generated to provide variability within populations and its quality management systems to ensure a robust and reproducible system is maintained.

1.2 PBPK Modelling and Simulation Report

The White Paper provides an overview of the modelling and simulation carried out to complete the proof of concept. However, full details of the IVIVE-PBPK model development and verification using the Simcyp population based simulator platform can be found in the modelling and simulation report (Burt, 2017). This report is intended as a companion to the White paper providing greater detail where required to support understanding and validation of the overall approach.

1.3 Supporting Documentation – Relevant Simcyp & White Paper References

The references quoted in the white paper that allow greater insight into the Simcyp simulator platform history and construction, key algorithms used in the software, how individuals are generated to provide variability within populations and its quality management systems to ensure a robust and reproducible system is maintained are provided. Appropriate copyright permission to supply these documents has been obtained by Simcyp.

1.4 Supporting Documentation – Simcyp Input and Output Files

For each of the scenarios simulated in rat, healthy human population, children aged 1 to 2 years and severely renally impaired populations the Simcyp output files are provided. These are in excel format and can be read without the need to access Simcyp. Note, these files also contain all the input information used by the models for simulation purposes.

The actual Simcyp workfiles for the scenarios simulated are also provided and can be used to re-run the simulations within Simcyp if desired. As stated above the Simcyp platform software can be provided to SAP panel members if requested.

Where the R-Simcyp package was used to aid simulations the R script is also listed and supplied.

Further details on the content of each file included are given in Appendix 2.

1.5 Supporting Documentation – *In Vitro* and *In Vivo* Study Reports

The proof of concept study is based around acibenzolar-S- methyl and a parallelogram approach to build and verify the IVIVE-PBPK models employed. The study reports detailing the generation of the *in vivo* rat and rat and human *in vitro* data have been made available for review.

2 Executive Summary

Human health risk assessments have traditionally used uncertainty factors to account for poorly quantified influences such as interspecies differences and population variability. Newer tools such as physiologically based pharmacokinetic (PBPK) modelling, *in vitro* to *in vivo* extrapolation (IVIVE) and human population simulation, can be used to provide quantitative estimates of human internal dose. A proof of concept study is presented using the fungicide acibenzolar-S-methyl (acibenzolar) as an exemplar compound to demonstrate how a population-based IVIVE-PBPK modelling approach can be employed to obtain data derived extrapolation factors (DDEFs) to improve human health risk assessments.

Rat and human population based IVIVE-PBPK models were developed from rat *in vivo* studies together with rat and human *in vitro*, absorption, distribution, metabolism, and excretion (ADME) assessments. The model allows a quantitative examination of interspecies extrapolation and human intraspecies variability (subpopulations), specifically to include at risk populations. Comparisons are made via the internal systemic dose, quantified by the area under the blood concentration-time curve (AUC). This approach supports traditional human health risk assessments based on acceptable margins of exposures relative to an external dose, and it also enables a ‘toxicokinetic safety margin’ to be defined based upon multiples of internal systemic dose relative to that at the human equivalent dose. The conclusion of this paper provides example human health dietary risk assessments in adults, children and renally impaired adults based on human equivalent dose, DDEFs and dietary exposure modelling.

3 Introduction

Human health risk assessment of agrochemicals typically involves the use of animal derived points of departure and the application of default uncertainty factors. The default 100-fold uncertainty factor is subdivided to recognize differences between the toxicology species and humans (10-fold) and variability within the human population (10-fold). These can be further subdivided to take into account variability in toxicokinetics (TK) and toxicodynamics (TD) as advocated by the WHO International Programme on Chemical Safety (IPCS) project on the harmonization of approaches to the assessment of risk from exposure to chemicals (WHO 2005) and shown in figure 2.

To reduce uncertainty and increase the scientific basis of risk assessments the IPCS report (WHO 2005) encourages the use of TK data to derive chemical specific adjustment factors, as does the EPA guidance for applying quantitative data to develop data derived extrapolation factors (DDEFs) for interspecies and intraspecies extrapolation (US EPA 2014). In setting out how quantitative DDEFs can be employed in a risk assessment, and to distinguish them from ‘uncertainty factors’, DDEFs addressing toxicokinetic and toxicodynamic differences between species (animal to human) and within species (human) have been termed EF_{AK} , EF_{AD} , EF_{HK} and EF_{HD} corresponding to AK_{UF} , AD_{UF} , HK_{UF} and HD_{UF} , respectively, as shown in figure 2. However, the US EPA use a one half order of magnitude (3.16) uncertainty factor across interspecies as well as intraspecies differences in TK and TD.

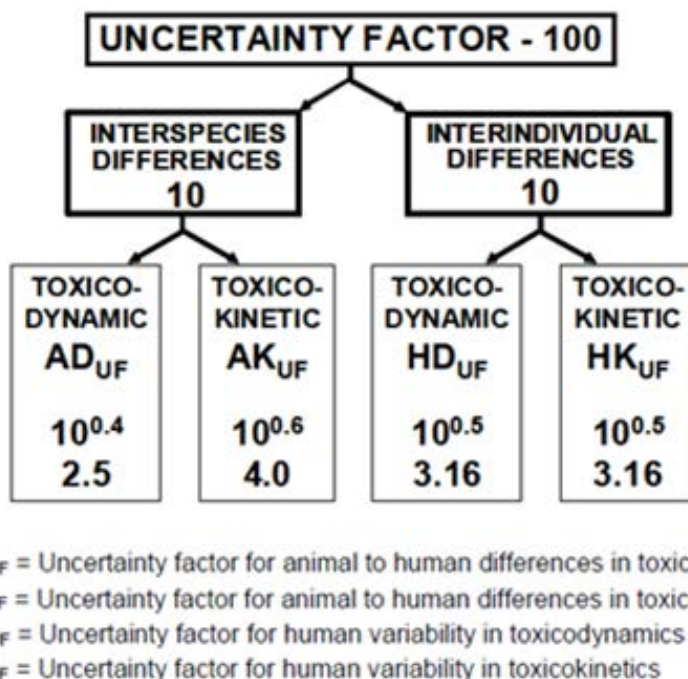


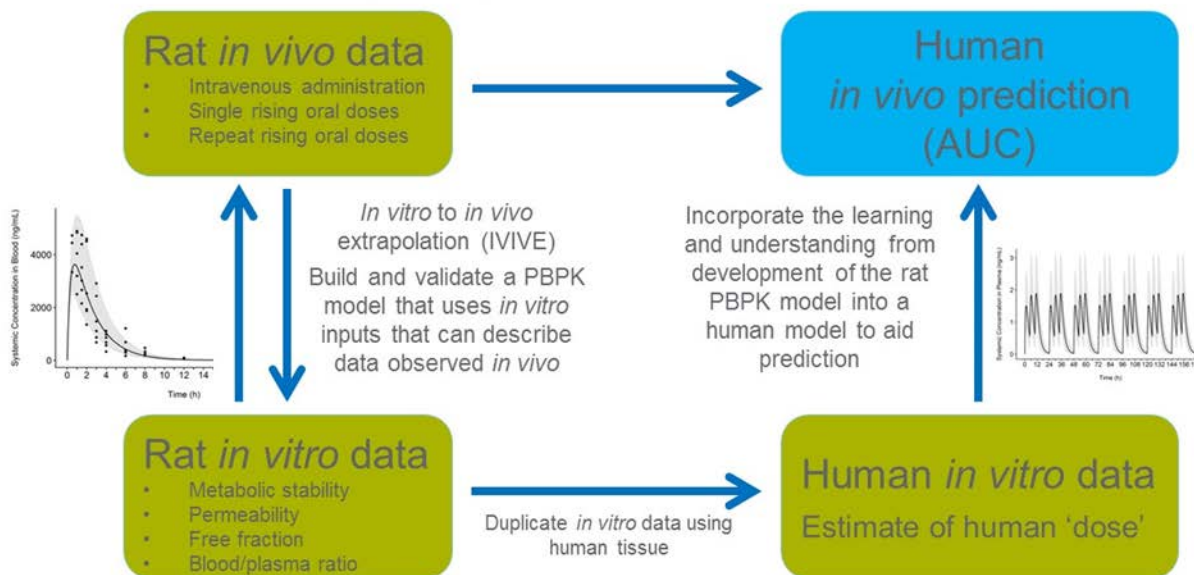
Figure 2: Subdivision of the default uncertainty factor of 100 reproduced from the World Health Organization (2005) used as guidance for setting the exposure limits of the general population such as ADIs, TDIs or RfDs. The US EPA use a one half order of magnitude uncertainty factor of 3.16 across interspecies and intraspecies differences in TK and TD defining the uncertainty factors as EF_{AK} , EF_{AD} , EF_{HK} and EF_{HD} (US EPA 2014) which are analogous to AK_{UF} , AD_{UF} , HK_{UF} and HD_{UF} .

The approach outlined in this white paper addresses toxicokinetic uncertainty (AK_{UF} and HK_{UF}) only. Therefore, for this proof of concept, the default subdivision of toxicodynamics as used by the US EPA was utilized where the default AD_{UF} is 3.16 and the default HD_{UF} is 3.16 giving a combined toxicodynamic uncertainty factor (UF_{TD}) of 10.

Obtaining toxicokinetic data to describe internal dosimetry within toxicology species is becoming more routine within the agrochemical industry (Creton, Billington *et al.* 2009; Creton, Saghir *et al.* 2012); however, in the agricultural industry, toxicokinetic data in humans is rarely collected due to barriers in study conduct and data acceptance by regulatory authorities.

One way to mitigate the lack of human *in vivo* TK data is to predict human internal dosimetry through the use of *in vitro* to *in vivo* extrapolation (IVIVE) and verifying by employing, what is often called, a ‘parallelogram approach’ (figure 3).

In Vitro Based Parallelogram Approach



Premise - if we can predict internal dosimetry *in vivo* from *in vitro* data in rat, using human *in vitro* data and an informed PBPK model we can predict human *in vivo* internal dosimetry

Figure 3: The parallelogram approach using IVIVE to predict human internal dosimetry

By using available *in vitro* and *in vivo* toxicokinetic data from animal species, such as the rat, a PBPK model is built that employs compound specific *in vitro* inputs to demonstrate that understanding of the TK of a test compound *in vivo* can be successfully obtained using *in vitro* data. By taking the learnings gained from development of the rat model, a human *in vivo* PBPK model is developed that uses human *in vitro* data as the inputs. TK simulations of human *in vivo* internal dosimetry under different scenarios could then be run and the output used as the basis on which to derive DDEFs to reduce uncertainty in human health risk assessments. This approach supports the development of human relevant data while minimizes the need for *in vivo* studies.

PBPK modelling and the IVIVE approach is typically used to generate a DDEF for toxicokinetic differences between test species and humans (*i.e.* EF_{AK}) by predicting the internal dosimetry of ‘a typical human individual’. This allows one default uncertainty factor to be replaced with a data derived factor. However, for this approach to be more broadly applied, and not just pertinent to reducing uncertainty in interspecies TK differences, the variability within the general adult human population must be described to define intraspecies extrapolation factors (EF_{HK}). In addition, the internal dosimetry in potentially sensitive or at risk sub-populations, such as children should also be defined to extend the risk assessment beyond the general population.

The human equivalent dose (HED) is the dose in humans that corresponds to the point of departure in animal test species and is used as the reference point in human health risk assessments. When field based residue data are available consumer consumption databases can be used to model human dietary ‘external’ exposure in various populations and derive a human “administered external dose”. By being in a position to simulate internal dosimetry within human populations at both the HED and also that following different consumer scenarios the internal dose metric, quantified by the area under the concentration-time curve (AUC), can be compared giving an alternative way to represent a risk assessment in terms of a ‘Toxicokinetic Safety Margin (TSM)’ as shown in figure 4.

Visualisation of Human Intraspecies Variability in AUC and Apparent Toxicokinetic Safety Margin (AUC at HED vs Consumer)

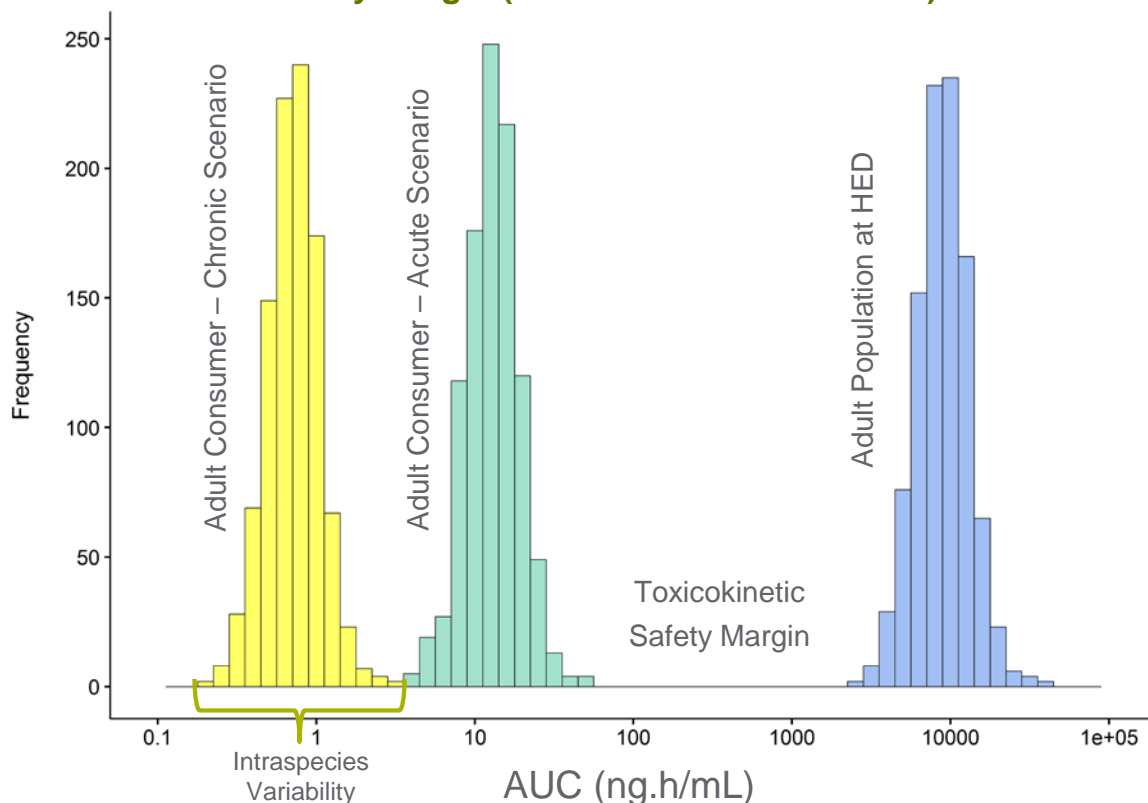


Figure 4: Example histogram showing comparison of the simulated AUCs at the human equivalent dose (blue bars) and after acute (green bars) and chronic (yellow bars) consumer dosing in adult humans to demonstrate a ‘toxicokinetic safety margin’.

Implementing such an approach to derive DDEFs or to define a ‘toxicokinetic safety margin’ would reduce uncertainty in risk assessments and move forward towards the goal of maximizing the use of available data and improving the overall scientific basis of a human health risk assessment.

Employing a population based IVIVE-PBPK modelling and simulation approach to reduce uncertainty in human health risk assessments in the Agrochemical regulatory environment would at present appear to be a complex and time consuming task requiring the development of novel modelling and simulation tools acceptable to regulators. However, to carry out a proof of concept study to demonstrate the utility of the approach and start the discussion on what a regulatory acceptable tool must deliver, options are available.

The ‘Simcyp Population-based Simulator’ contains extensive demographic, physiologic and genomic databases which are incorporated into algorithms that generate clearly defined individuals creating a virtual population that can be submitted to ‘a clinical trial’ thereby allowing human TK variability within the population to be described. It has become established within the pharmaceutical industry and is recognized and used by regulators as part of the regulatory process.

As such, Simcyp presented us with a viable, readily available tool with which to carry out a ‘proof of concept’ study for the approach described above and forms the basis of the submission to the SAP.

4 The Simcyp Population Based Simulator Platform

4.1 General Background

The Simcyp Population-based ADME Simulator is a platform and database for mechanistic modelling and simulation of the processes of oral absorption, tissue distribution, metabolism and excretion of drugs and drug candidates in healthy human and disease populations (categorized by age, disease, race), and for predicting the extent of metabolically-based drug–drug interactions. In the context of systems PK, the Simulator combines experimental data generated routinely during preclinical drug discovery and development from *in vitro* enzyme and cellular systems and relevant physicochemical attributes of compound and dosage form with demographic, physiological and genetic information on different patient populations to predict *in vivo* PK parameters and profiles. An overview of the framework and organisation of the Simulator and how it combines different categories of information has been described by Jamei et al (2009).

In the case of the Simcyp animal Simulators (rat, mouse, dog and monkey) variability is only incorporated for a limited number of specific model aspects and, by default, there is no variability incorporated into any aspects of the rat and mouse Simulators. Therefore, when default simulations are performed in these species a single PBPK model is generated with average attributes for the species applied.

The initial focus of the Simulator was mechanistic *in vitro* – *in vivo* extrapolation to predict drug clearance and the extent of metabolic drug–drug interactions (mDDI) at steady-state (Rostami-Hodjegan and Tucker, 2007). This has now been extended to the prediction of full concentration time-profiles. At present, the Simulator addresses all aspects of ADME prediction including drug absorption (Rostami-Hodjegan, 2012; Jones and Rowland, 2013).

Recent architectural and implementation developments within the Simulator have been published (Jamei et al, 2013). This article includes details of interconnection between peripheral modules, the dynamic model building process and compound and population data handling. The Simcyp Data Management (SDM) system, which contains the system and drug databases and helps with implementing quality standards by seamless integration and tracking of any changes is also described. This also helps with internal approval procedures, validation and auto-testing of the new implemented models and algorithms, an area of high interest to regulatory bodies.

PBPK models using nonclinical and clinical data to predict drug PK/PD properties in healthy and patient subjects are increasingly used at various stages of drug development and regulatory interactions. However, initially the regulatory applications of PBPK models were mainly focused on predicting DDI, the areas of application are gradually expanding. These are expanded in other areas such as drug formulation and/or absorption modelling, age- and ethnic-related changes in PK and disposition (e.g. paediatrics/geriatrics and Japanese/Chinese populations) and the assessment of PK changes in case of different physiopathological conditions (e.g. renal and/or hepatic deficiencies).

Recently, a number of drug labels have been informed by simulation results generated using PBPK models. These cases show that either the simulations are used in lieu of conducting clinical studies or have informed the drug label that otherwise would have been silent in some specific situations. A summary of the impact of PBPK on regulatory decisions and drug labels has been published (Jamei, 2016).

4.2 Simcyp Version and Base PBPK Model

The Simcyp Rat Simulator (Version 15) was used (www.simcyp.com) for all rat model development and simulations. Minimal physiologically-based pharmacokinetic (PBPK) models, which consider metabolism in both the liver and intestine, and lump all other tissues into the systemic compartment, were developed for both acibenzolar and its metabolite acibenzolar-acid (Figure 5 and Section 3.1.1 in Burt 2017).

The human Simcyp Population-based Simulator (Version 15) was used (www.simcyp.com) for all human model development and simulations. The structure of the human model is unchanged from the rat model, only the parameterization is different.

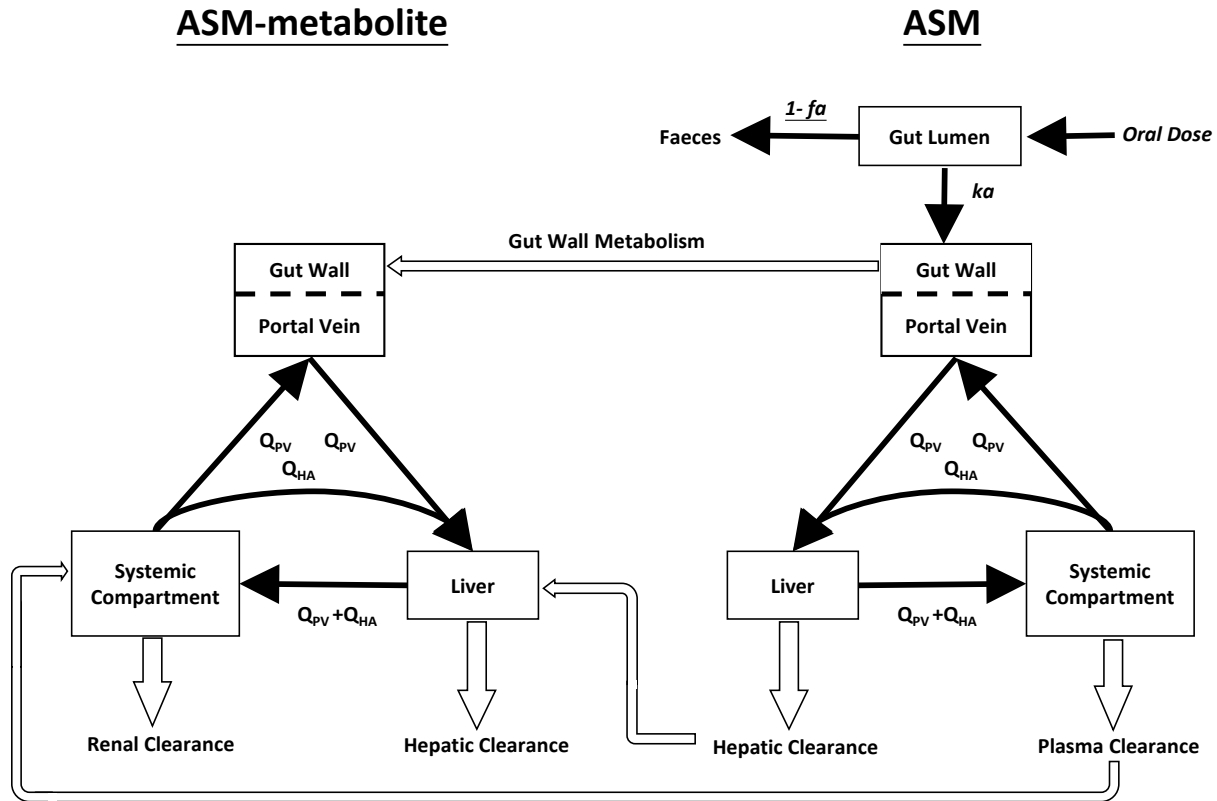


Figure 5. The minimal physiologically based pharmacokinetic models for acibenzolar and acibenzolar-acid. Q_{pv} , and Q_{ha} are blood flows in the portal vein and hepatic artery, respectively; ka is the first order absorption rate constant and fa is the fraction absorbed.

The metabolism of acibenzolar at different locations in the acibenzolar model results in the corresponding formation of acibenzolar-acid at the same location.

The models are defined by Equation 4.1 to Equation 4.3 (Rowland Yeo et al., 2010 and Section 3.3.1 in Burt 2017).

$$C_{pv} = \frac{Q_{pv} \times C_p \times B/P + fa \times F_G \times ka \times Dose \times \exp(-ka \times t)}{Q_{pv} \times B/P}$$

Equation 4.1

Where C_{pv} is the concentration of compound in the portal vein blood, C_p is the systemic concentration of compound in plasma, B/P is the blood to plasma ratio of compound, fa is the fraction of drug absorbed, F_G is the fraction of compound which escapes first-pass metabolism in the intestine, ka is the absorption rate constant and Q_{pv} is the portal vein blood flow.

$$\frac{dC_{Liv}}{dt} = \frac{1}{V_{Liv}} \left(-Q_{Liv} \times \frac{C_{Liv}}{K_p} \times B/P + Q_{pv} C_{pv} \times B/P + Q_{ha} C_p \times B/P - CL_{u_{int-H}} \times C_{u_{Liv}} \right)$$

Equation 4.2

Where C_{Liv} and $C_{u_{Liv}}$ are the total and unbound concentrations of compound in the liver, K_p is the liver to plasma partition coefficient, $CL_{u_{int-H}}$ is the scaled unbound intrinsic clearance of compound in the liver, Q_{ha} is hepatic artery blood flow, Q_{Liv} is liver blood flow ($Q_{ha} + Q_{pv}$) and V_{Liv} is the volume of the liver.

$$\frac{dC_p}{dt} = \frac{1}{(V_{ss} - (V_{Liv} \times K_p))} \left(Q_{Liv} \times \frac{C_{Liv}}{K_p} \times B/P - (Q_{pv} + Q_{ha}) \times C_p \times B/P - (CL_R + CL_P) \times C_p \right)$$

Equation 4.3

Where CL_R and CL_P are renal and plasma clearances, respectively and V_{ss} is the steady state volume of distribution.

4.3 Building Virtual Individuals

When simulations are conducted within the human Simcyp Simulator, virtual individuals are created on the basis of complex covariate relationships established from meta-analysis of data in the scientific literature. A schematic overview of the relationships within the human Simcyp Simulator is provided in Figure 6 reproduced from Jamei et al. (2009).

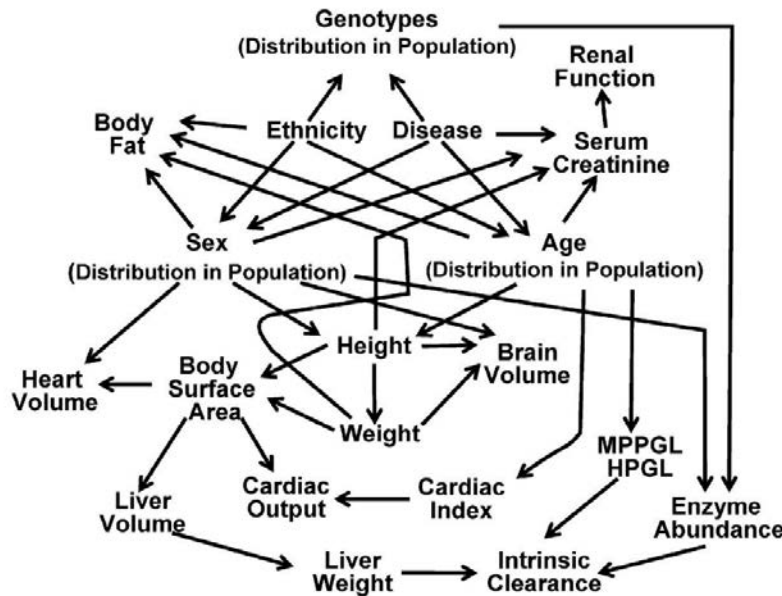


Figure 6. When building virtual human populations for ADME simulation, the composition of the study group is initially considered with respect to age, sex and ethnicity, plus the genetic makeup of enzymes and transporter proteins in the target population. However, each of these factors influences multiple elements of ADME creating highly non-linear and non-monotonic relationships.

Once individualised parameters are generated, these are used to build the PBPK model for each individual. As an example, when scaling an *in vitro* intrinsic clearance determined in human liver microsomes into a corresponding *in vivo* intrinsic clearance to be applied within a PBPK model, Equation 4.4 can be used in order to obtain an intrinsic clearance for each individual. In this case, the milligrams of protein per gram of liver (MPPGL) and liver weight for the individual will be applied.

$$CLu_{int-H} = \frac{V_{max}}{K_m \cdot fu_{inc} + Cu_{Liv}} \cdot MPPGL \cdot LW \cdot 60/10^3$$

Equation 4.4

Where CLu_{int-H} (L/h) is the unbound intrinsic clearance in the liver, V_{max} (nmol/min/mg microsomal protein) and K_m (μ M) are the maximum rate of metabolism and Michaelis constant determined *in vitro*, respectively, Cu_{Liv} is the unbound concentration in the liver determined on each time-step within the PBPK model, fu_{inc} is the corresponding fraction unbound in the *in vitro* experiment, $MPPGL$ is the microsomal protein per gram of liver (mg/g) and LW is the liver weight (g). The term $60/10^3$ is for unit conversion.

5 IVIVE-PBPK Proof of Concept Objectives

This white paper sets out the ‘proof of concept’ study carried out to demonstrate how a population based IVIVE-PBPK modelling and simulation approach can predict internal dosimetry within a human population and the outputs implemented into reducing uncertainty in a human health risk assessment. Specifically for this study, a model compound (Acibenzolar-S-Methyl) and the Simcyp population based simulator platform were used.

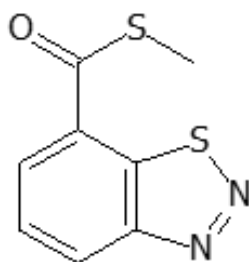
In presenting this proof of concept study Syngenta attempts put this approach into a pesticide regulatory context and address the answers to the following questions:

1. Is the proposed population based IVIVE-PBPK modelling and simulation approach employed scientifically justified to provide predictions of internal dosimetry in the specified human populations?
2. Could a toxicokinetic interspecies extrapolation factor (EF_{AK}) be reliably derived from the approach employed and used to reduce uncertainty in human health risk assessments?
3. Could a toxicokinetic intraspecies extrapolation factor taking into account variability within the human population (EF_{HK}) be reliably derived from the approach employed and used to reduce uncertainty in human health risk assessments?
4. Can a human health risk assessment be conducted by directly comparing the AUC in consumer populations to the AUC predicted at the human equivalent dose? This is referred to in the document as a “toxicokinetic safety margin”.

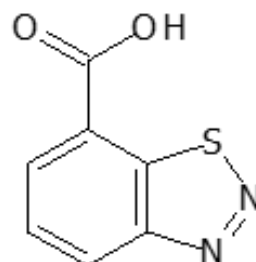
5. How, as part of a human health risk assessment, should consideration of the toxicological end point determining the POD or inclusion of default toxicodynamic uncertainty factors be used to put the toxicokinetic safety margin described above into context?
6. What are the critical criteria that must be met by a platform used to carry out a population based IVIVE-PBPK modelling & simulation approach that would provide sufficient ‘transparency’ to allow its acceptance and use to reduce uncertainty in human health risk assessments submitted for regulatory approval?
7. Is the Simcyp population based simulator platform used in this proof of concept study an acceptable umbrella under which to carry out such an approach?

6 Acibenzolar

The model compound chosen for the proof of concept study, acibenzolar-S-methyl (hereafter referred to as acibenzolar) is a fungicide and plant growth regulator labelled for suppression of bacterial spot, speck and control of blue mold.



Acibenzolar-S-Methyl
CSAA232020
(ASM)



Carboxylic acid metabolite
CSAA197129
(ASM-metabolite)

Acibenzolar-S-Methyl has been used in the case presented as an exemplar compound to provide a ‘proof of concept’ and has no registration issues in the USA that need to be addressed.

6.1 Synonyms

As stated above, in this white paper acibenzolar-S-methyl is being used to provide a proof of concept and is referred to as acibenzolar but, in supplementary reports and supporting documentation, the following synonyms have also been utilized: CSAA23200, CGA 245704, and ASM. The carboxylic acid metabolite of acibenzolar is referred to as acibenzolar-acid. In supplementary reports and supporting documentation this is also referred to as acibenzolar-acid, ASM-metabolite, CSAA197129 or CGA 210007.

6.2 Toxicity Endpoint & Point of Departure

6.2.1 Toxicity Endpoint

Acibenzolar has been evaluated in acute and repeat dose toxicity studies in rats, mice, rabbits and dogs, in developmental toxicity studies in rats and rabbits and reproductive toxicity and developmental neurotoxicity studies in rats (US EPA 2009a; PMRA 2010; US EPA 2012).

The lowest potential point of departure (POD) in the acibenzolar data base is 8.2 mg/kg taken from the rat developmental neurotoxicity study (DNT, Pinto 2002). Further details on acibenzolar toxicity end points and points of departure can be found in Appendix 1.

6.2.2 Point of Departure for Risk Assessment Purposes

To be conservative and consistent with existing regulatory opinion, 8.2 mg/kg has been used for both example acute and chronic dietary risk assessments for the purpose of demonstrating the utility of our approach.

6.3 Rat *In Vivo* Absorption, Distribution, Metabolism and Excretion

In rat *in vivo* studies using [¹⁴C] radiolabeled material, oral absorption of acibenzolar was > 90% (US EPA 2012). Acibenzolar is metabolized via rapid hydrolysis through nonspecific serum carboxylesterases to the carboxylic acid metabolite (acibenzolar-acid) as shown in *in vitro* studies with rat and human liver homogenates utilizing specific esterase inhibitors (Sagelsdorff and Buser, 1994). In an ADME study where an oral gavage dose of 0.5 or 100 mg/kg of [¹⁴C]-acibenzolar was administered (Molitor, 1995), excretion was essentially complete by 48 hours post dose with ~96% of the ¹⁴C dose recovered in urine and ~5% in feces. In urine no parent was detected with > 90% present as the carboxylic acid and < 2 % as a glycine conjugate of the carboxylic acid and < 4.5% was unknown. In feces the carboxylic acid predominated together with a small amount of parent and < 0.4% was unknown.

Due to the rapid conversion of acibenzolar to its metabolite (acibenzolar-acid) with no further metabolism, all concentration-time data used for the purpose of this submission is based on acibenzolar-acid.

The only toxicokinetic data available for acibenzolar at the time of starting this work was the radiolabeled study. Therefore, an additional toxicokinetic study was performed (Punler and Tomlinson, 2017) to provide data on acibenzolar and acibenzolar-acid for construction and verification of the rat PBPK model. This work is detailed in Section 9.

7 IVIVE-PBPK Modelling and Simulation Approach

The strategy to complete the proof of concept involved a stepwise approach as summarized in figure 7. The first step involved generation of the *in vitro* data generated to inform on absorption, distribution and metabolism that would be used to aid construction and be employed as input

parameters for the rat PBPK model (section 13). As the only previous PK data available was from an *in vivo* study where total radioactivity only was measured, an additional *in vivo* study was also conducted to provide TK data on acibenzolar and acibenzolar-acid to aid construction and verification of the rat model (section 9). The data from these *in vitro* and TK studies together with physico-chemical data were used to construct the rat PBPK model using the Simcyp platform.

The internal dosimetry of acibenzolar-acid and its associated variability in the study defining the POD was simulated using this model utilizing variability in appropriate parameters within the Simcyp simulator.

Human *in vitro* distribution and metabolism data were generated using human tissues. Using the knowledge gained from construction of the rat model, a human PBPK model for acibenzolar was constructed employing the *in vitro* human data as inputs in addition to some allometrically scaled parameters from the rat *in vivo* data. Human internal dosimetry and associated variability was simulated under various relevant scenarios (acute and chronic dietary consumer scenarios and potentially sensitive populations). The model construction and evaluation were conducted within the Simcyp simulator.

Internal dosimetry and associated variability in both the rat and human populations under various scenarios were then used to provide human equivalent doses (HED) and DDEFs. The difference in AUC resulting from external consumer exposure (dietary and water consumption) to AUC at the human equivalent dose to define a ‘toxicokinetic safety margin’ was also investigated.

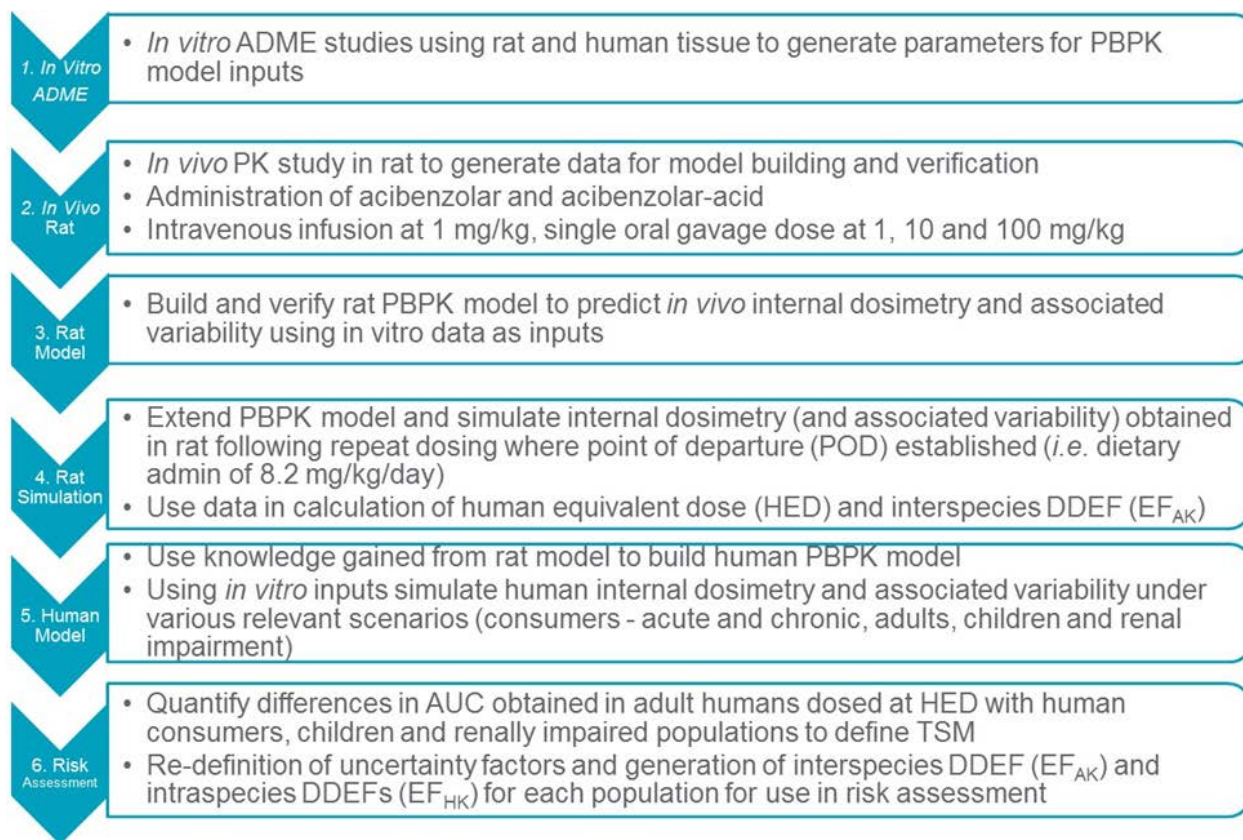


Figure 7: PBPK modelling and simulation approach employed to obtain TSMs and DDEFs

8 Acibenzolar *In Vitro* ADME Studies (Rat & Human)

8.1 *In Vitro* Investigations Carried Out

In order to provide input data for construction of the rat and human population based PBPK models, *in vitro* studies were required. Using hepatocytes, microsomes, plasma, blood, recombinant carboxylesterase enzymes (CES) and Caco-2 cells, *in vitro* absorption, distribution and metabolism data for acibenzolar and/or acibenzolar-acid were derived from K_m and V_{max} determination, buffer stability, hepatocyte stability, plasma stability, blood stability, microsomal binding, hepatocyte binding, plasma protein binding, blood binding, blood plasma ratio and Caco-2 permeability (including identification of efflux via P-gp and/or BCRP). Details and results from all of the *in vitro* studies can be found in Frost (2017).

The data utilized as input parameters for the distribution and metabolism parts of the PBPK model are summarized below and tabulated with physicochemical and *in vivo* PK inputs in section 12.

8.2 Free Fraction in Plasma & Blood to Plasma Ratios

The free fraction (f_u) of acibenzolar and acibenzolar-acid in rat and human plasma was determined by equilibrium dialysis. The experimentally determined f_u was used as input parameters for blood binding in the PBPK model and are shown in Table 1.

Table 1: Plasma free fractions (f_u) of acibenzolar and acibenzolar-acid in rat and human plasma

Species	Acibenzolar f_u	Acibenzolar-acid f_u
Human	0.0523	0.0206
Rat	0.0469	0.0739

A blood to plasma ratio for acibenzolar could not be determined *in vitro* due to rapid hydrolysis to acibenzolar-acid. For rat no QSAR model was available so it was assumed to be 1. For human a QSAR model is available within Simcyp which gave a prediction of 0.877. These were then used as input parameters to predict blood binding within the respective PBPK models.

The blood to plasma ratio for acibenzolar-acid was determined *in vitro* using an LC/MS/MS-based depletion method as detailed in Frost (2017). Blood to plasma ratios of 0.679 and 0.651 were determined for rat and human, respectively, and were subsequently used as input parameters for prediction of blood binding within the PBPK model.

8.3 *In Vitro* Metabolism

The metabolism of acibenzolar was defined from *in vitro* experiments whereby the kinetic parameters (V_{max} and K_m) for the formation of acibenzolar-acid were estimated for modelling purposes over a concentration range of 1 to 100 μM and were adequately described by a standard monophasic Michaelis-Menten model which could be readily applied by the PBPK model (Burt

2017). Metabolism data from experiments in cryopreserved rat hepatocytes, rat liver microsomes, rat intestinal microsomes and rat plasma were analyzed in this way and are reported in Appendix 1 in Burt (2017).

Hepatic metabolism of acibenzolar was represented in the PBPK model by the metabolism observed in hepatocytes. For the observed V_{max} to be incorporated into the PBPK model as hepatic esterase metabolism it was converted to a microsomal equivalent using hepatocyte and microsomal scaling factors using equation 8.1 (also described in Section 3.1.1.3 in Burt 2017).

$$V_{max,microsomes} = V_{max,hepatocytes} \cdot \frac{HPGL}{MPPGL}$$

Equation 8.1

Where HPGL is the number of hepatocytes per gram of liver (108 million cells/g liver) and MPPGL is the amount of microsomal protein per gram of liver (46 mg protein/g liver).

Intestinal metabolism of acibenzolar was represented in the PBPK model by the metabolism in intestinal microsomes. The observed V_{max} was converted to an equivalent whole cell (enterocyte) metabolism based on the difference in the V_{max} between rat liver microsomes and rat hepatocytes, assuming a similar distribution of these enzymes in enterocytes as in the liver using equation 8.2 (also described in Section 3.1.1.3 in Burt 2017).

$$V_{max,enterocytes} = V_{max,intestinal\ microsomes} \cdot \frac{V_{max,hepatocytes} \cdot HPGL}{V_{max,liver\ microsomes} \cdot MPPGL}$$

Equation 8.2

Where $V_{max,enterocytes}$ and $V_{max,intestinal\ microsomes}$ are the theoretical enterocyte and intestinal microsomal V_{max} (nmol/min/mg protein) respectively, $V_{max,hepatocytes}$ and $V_{max,liver\ microsomes}$ are the hepatocyte (nmol/min/million cells) and liver microsomal (nmol/min/mg protein) V_{max} , respectively.

The calculated esterase equivalent V_{max} and K_m estimates for liver and the enterocyte V_{max} and K_m estimates for intestine were input into the PBPK model where they were converted to an intrinsic clearance in the liver and intestine as detailed in Equation 13.2 and in Section 3.1.1.3 in Burt (2017).

Within these calculations, the extent of non-specific binding of acibenzolar to the different matrices was taken into account. These were determined experimentally via equilibrium dialysis and are shown in Table 2 along with the V_{max} and K_m used as PBPK model inputs.

Table 2: V_{max} , K_m and non-specific binding ($f_{u_{inc}}$) input parameters for acibenzolar metabolism

Matrix	Species	V_{max} (nmol/min/mg protein)	K_m (uM)	$f_{u_{inc}}$
Hepatocyte	Rat	519	69	0.919
	Human	1473	92	0.982
Intestine	Rat	134	117	0.877*
	Human	38	311	0.252*

*non-specific binding was assumed to be equivalent for liver and intestinal microsomes therefore liver microsomal data was used for intestinal non-specific binding and in the case of human was corrected for the difference in protein concentration between binding and kinetic experiments

Plasma metabolism of acibenzolar was represented in the PBPK model as a half-life which was based on the intrinsic clearance in plasma (V_{max}/K_m) and the volume of plasma in the experiment. Half-lives of 13.4 and 252 minutes were determined using this method for rat and human, respectively. These were then used as the input parameters in the PBPK model in the oral dosing scenarios.

Acibenzolar-acid was essentially stable in human and rat hepatocytes with hepatic intrinsic clearances of 0 and 0.596 uL/min/million cells, respectively. Non-specific binding ($f_{u_{inc}}$) of acibenzolar-acid to hepatocytes was 0.946. These were also used as input parameters for acibenzolar-acid hepatic metabolism in the PBPK model.

9 Acibenzolar *In Vivo* Studies in Rat

9.1 *In Vivo* Toxicokinetic Study Design

As part of the parallelogram approach *in vivo* studies were carried out in rat to aid PBPK model building and verification. Based on the information from the ^{14}C study described above (section 6.3), dosing of non-radiolabeled acibenzolar with TK monitoring of both acibenzolar and acibenzolar-acid was considered to be sufficient to describe the internal dosimetry in the rat. Therefore, an *in vivo* study dosing acibenzolar and/or acibenzolar-acid monitoring for formation of the acibenzolar-acid was performed (Punler and Tomlinson, 2017). In this study the urinary recovery of acibenzolar-acid was used for confirmation of complete conversion to the metabolite and determination of renal clearance.

Doses were selected to cover a range around the toxicity POD to allow for determination of any non-linearity in the toxicokinetics. The studies are summarized below and full study information and data can be found in Punler and Tomlinson (2017).

Preliminary phases of the study demonstrated that the internal dosimetry of acibenzolar-acid was equivalent following intravenous infusion of acibenzolar or acibenzolar-acid itself. Therefore, in the main phases of the study that were used to derive toxicokinetic parameters for construction and verification of the PBPK model, acibenzolar was dosed and the internal dosimetry of acibenzolar and acibenzolar-acid was determined.

Six female Han Wistar rats received a single administration of acibenzolar at 1 mg/kg as a constant rate intravenous infusion over 1 hour. Serial blood samples were taken from n=6 animals. Three of the animals were also placed in metabowls to allow for the quantitative collection of urine. In the second phase of the study, 6 female Han Wistar rats received a single oral administration of acibenzolar at 1, 10 or 100 mg/kg and samples were taken as for the intravenous phase. Blood and urine samples were analyzed for concentration of acibenzolar and/or acibenzolar-acid. The pharmacokinetic parameters derived from the concentration-time data are summarized below in Table 3 and Table 4.

9.2 *In Vivo* Toxicokinetic Study Results

In summary, metabolism of acibenzolar to acibenzolar-acid was so rapid such that acibenzolar internal dosimetry was not well characterized and any pharmacokinetic analysis was limited. However, concentration-time profiles of acibenzolar-acid obtained following intravenous infusion of either acibenzolar or acibenzolar-acid itself were effectively superimposable. Following intravenous infusion, metabolism of acibenzolar to acibenzolar-acid was also complete with >90 % of the dose recovered as acibenzolar-acid in urine.

Similarly, following oral administration of acibenzolar, the fraction of the dose excreted in urine (f_e) as acibenzolar-acid was essentially complete following 1 and 10 mg/kg indicating that oral bioavailability of acibenzolar was 100% within this dose range. These findings are consistent with the previous ^{14}C study (Molitor 1995) and demonstrate that concentrating on the internal dosimetry of the acibenzolar-acid metabolite was the correct path to follow. With this information in hand, pharmacokinetic parameters were calculated using non-compartmental analysis for acibenzolar-acid. This described the disposition and absorption following administration of acibenzolar with the dose adjusted using the molecular weight acid/parent ratio and these are also summarized in Table 3 and Table 4 below.

The clearance of acibenzolar-acid was calculated using Equation 9.1 assuming complete conversion of absorbed acibenzolar.

$$CL_{ASM-metabolite} = \frac{Dose_{ASM} \cdot fa_{ASM} \cdot MW_{t_{ASM-metabolite}}}{AUC_{ASM-metabolite} \cdot MW_{t_{ASM}}}$$

Equation 9.1

Where $Dose_{ASM}$ is the actual (not nominal) dose of acibenzolar (mg/kg), fa_{ASM} is the fraction of acibenzolar absorbed (1 in the case of intravenous dosing), $AUC_{ASM-metabolite}$ is the $AUC_{(0,t)}$ of acibenzolar-acid (mg/mL.h) and $CL_{ASM-metabolite}$ is the clearance of acibenzolar-acid (mL/h/kg).

9.2.1 Intravenous Dose Toxicokinetics (1 mg/kg)

Table 3: Mean ± sd (n=6) Acibenzolar and Acibenzolar-Acid Pharmacokinetic Parameters Following Intravenous Infusion of 1 mg Acibenzolar/kg to Female Rats.

PK Parameter	Units	Acibenzolar Mean ± SD	Acibenzolar-acid Mean ± SD
C _{max}	ng/mL	19.1±3.87	735±152
T _{max} ^A	h	0.667 (0.667 – 1)	0.833 (0.667 – 1)
T _{1/2}	h	-	1.13±0.612
AUC _{last}	ng.h/mL	12.1±4.63	780±163
AUC _{inf}	ng.h/mL	-	840±177
AUC extrapolated	%	-	1.64±1.11
CL	mL/h/kg	-	1140±303
fe	% dose in urine	-	89.5
CLr	mL/h/kg	-	913±184
V _{ss}	mL/kg	-	1520±530

Note: CL and V_{ss} of acibenzolar-acid have been calculated following acibenzolar administration on the basis that all acibenzolar was rapidly and completely converted to acibenzolar-acid and using equivalent dose (mg/kg) corrected using MW acid/parent ratio.
 Note II: Renal Clearance (CLr) was calculated for acibenzolar-acid based upon recovery in urine and AUC in blood following administration of acibenzolar. Majority of urine acibenzolar concentrations were below the limit of quantification therefore CLr could not be determined.
 - A terminal phase was not characterized. ^A Median and range for t_{max}.

9.2.2 Oral Dose Toxicokinetics (1, 10 and 100 mg/kg)

Table 4: Mean ± sd (n=6) Acibenzolar-acid Pharmacokinetic Parameters in Blood Following Oral Administration of 1, 10 or 100 mg Acibenzolar/kg to Female Rats.

PK Parameter	Units	1 mg/kg Mean ± SD	10 mg/kg Mean ± SD	100 mg/kg Mean ± SD
C _{max}	ng/mL	762±287	4430±782	23900±5470
T _{max} ^A	h	0.5 (0.5 - 1.5)	0.5 (0.5 – 1)	3 (1.5 – 4)
T _{1/2}	h	3.09±3.01	7.31±5.35	10.4
AUC _{last}	ng.h/mL	1240±822	13600±3620	130000±11600
AUC _{inf}	ng.h/mL	1280±921	14600±3040	117000
AUC extrapolated	%	3.52±3.01	0.671±0.593	0.163
CL/F	mL/h/kg	989±509	676±147	824
fe	% dose in urine	91.2	84.2	53.4
CLr	mL/h/kg	984±584	505±159	427
V _{ss}	mL/kg	2140±897	2820±1590	4650

Note: CL/F and V_{ss} for acibenzolar-acid have been calculated using equivalent dose (mg/kg) corrected using MW acid/parent ratio.
 Note II: Renal Clearance (CLr) was calculated for acibenzolar-acid based upon recovery in urine and AUC in blood. All urine acibenzolar concentrations were below the limit of quantification. CLr = (total amount excreted/AUC(0-t))/animal weight, ^A Median and range for t_{max}.

From these data, the calculated renal clearance for acibenzolar-acid was corrected for blood to plasma ratio to give a plasma renal clearance and this was input directly into the rat PBPK model.

The absorption (k_a), volume of distribution (V_{ss}) and the plasma half-life following IV dosing of acibenzolar were derived by fitting the rat PBPK model to the *in vivo* concentration-time data using the parameter estimation module within the Simulator.

K_a and V_{ss} were scaled via allometry for use in the human PBPK model (section 13.1.1 and 13.1.2), whereas the slower experimental half-life determined in human plasma was applied in order to represent a worst case scenario.

The final input parameters derived from the *in vivo* data along with physicochemical data and *in vitro* inputs for the rat and human PBPK models are tabulated and shown in section 13.

The *in vivo* rat PK parameters derived via non-compartmental analysis detailed in Tables 3 and 4 were used to verify outputs from the rat PBPK model.

10 Consumer Exposure to Acibenzolar via Food and Drinking Water

Food and drinking water intake are key exposure pathways of aggregate exposure (*i.e.* external dose). To estimate the external dose from food and drinking water we (Syngenta) have used the Dietary Exposure Evaluation Model (DEEM-FCID Version 4.02) from EPA with 2005-2010 What We Eat in America (WWEIA), National Health and the Nutrition Examination Survey (NHANES) consumption database.

Acibenzolar is registered on tomatoes and tobacco in Canada and import tolerances established for leafy vegetables, brassica vegetables, fruiting vegetables, tomato paste and bananas. PMRA's dietary exposure assessment which included all the above crop uses served as a baseline for the food assessment (PMRA 2010).

The analysis incorporated Canadian MRLs/US Tolerances (US EPA 2009a and 2009b), median residues (STMdRs) from field trials, refined percent crop treated, experimentally determined processing factors and monitoring data. Acibenzolar residues from a proposed apple use (US EPA 2012) were also considered and exposures calculated using factor and monitoring data. These estimates were included in the dietary exposure calculations.

Estimated drinking water concentration (EDWC) was derived using the surface water module in PWC (Pesticide in Water Calculator) model. The generated EDWCs assumed that acibenzolar was applied at a rate of 449 g ai/ha/year (0.4 lb ai/A/year) to bare soil as a worst case.

Food and drinking water exposures were summed to provide the aggregate exposures for each relevant population subgroup. The acute dietary (food and drinking water) exposure assessment was a refined Tier III assessment; therefore, the combined food and drinking water exposures at the 99.9th percentile were reported for each population subgroup and are shown below as dietary exposure in mg/kg/day. Both acute and chronic exposure scenarios are summarized in Table 5.

Table 5: Acute and Chronic Dietary (Food, Drinking Water and Aggregate) Exposures

Population Subgroup	Acute Dietary Exposures (mg/kg/day)			Chronic Dietary Exposures (mg/kg/day)		
	Food	Water	Aggregate	Food	Water	Aggregate
General U.S. Population	0.001717	0.001108	0.002825	0.000133	0.000024	0.000157
All Infants (<1 year)	0.001804	0.002097	0.003901	0.000524	0.000090	0.000614
Children 1-2 years	0.003456	0.001847	0.005303	0.000945	0.000033	0.000978
Children 3-5 years	0.003182	0.000964	0.004146	0.000643	0.000027	0.000670
Children 6-12 years	0.001720	0.000804	0.002524	0.000206	0.000020	0.000226
Youth 13-19 years	0.001147	0.000649	0.001796	0.000083	0.000017	0.000100
Adults 20-49 years	0.001255	0.000682	0.001937	0.000067	0.000024	0.000091
Adults 50+ years	0.001453	0.000698	0.002151	0.000067	0.000023	0.000090
Females 13-29 years	0.001276	0.000711	0.001987	0.000068	0.000023	0.000091

11 Identification of Potentially ‘At Risk’ Populations

The population subgroup with the highest estimated acute and chronic dietary exposures is children 1-2 years old (Table 5) and, therefore, was chosen as an exemplar potential ‘at risk’ population to simulate using the PBPK model and for whom to define specific DDEFs and a TSM to include in exemplar risk assessments.

In addition, as acibenzolar-acid is a renally cleared compound, adults with renal impairment could also be identified as being an ‘at risk’ population and so were also included in the simulations as an additional population. For these subjects it was assumed that the renally impaired populations (moderate and severe renal impairment) were exposed to acibenzolar to the same extent as the general US population.

12 Doses for Simulation of Acute and Chronic Exposure Scenarios

For the simulations using the human PBPK model it was assumed bioaccessability of acibenzolar from food and water was 100% and chronic exposure was divided equally between 3 external doses equating to meal times taken at 7 am, 12 noon and 5 pm.

The acute (single dose) and chronic (3 doses/day) scenarios used in the simulations of human TK in adults (healthy and renally impaired) and children aged 1 – 2 years to characterize intra-species variability are outlined in table 6.

Table 6: Human dietary consumption/external doses of acibenzolar used for PBPK model simulations

Scenario	Adult	Children (1-2 years)
Acute Dose	0.002825 mg/kg	0.005303 mg/kg
Chronic Dose	0.000157 mg/kg/day 0.0000523 mg/kg (each dose) ¹	0.000978 mg/kg/day 0.000326 mg/kg (each dose) ¹

¹ chronic dose divided into 3 equal doses and simulated equating to meal times taken at 7 am, 12 noon and 5 pm.

13 Development, Verification and Output of Rat and Human PBPK Modelling and Simulation

Our approach utilizes two different and distinct portions of the Simcyp simulator platform:

1. population simulator to describe the populations of interest and
2. PBPK model tool to simulate the TK in these populations.

The development of the rat and human PBPK models, model verification and outputs are fully described in the companion report included with this submission (Burt, 2017) and are summarized below.

13.1 Rat PBPK Model

The rat PBPK models for acibenzolar and acibenzolar-acid were generated based on the available physicochemical, plasma binding and *in vitro* metabolism data in addition to the rat PK data obtained following intravenous and oral dosing as described in sections 8 and 9 (Frost 2017, Punler and Tomlinson 2017) and is summarized below. The final input parameters are shown in Tables 7 and 8 with more details of how they were obtained/derived available in Section 3.1 of Burt (2017). For input into Simcyp, the parameters (e.g., half life, renal clearance) are required to be with respect to plasma. The output parameters are all reported with respect to blood having been corrected for blood to plasma ratio within the simulator.

These models were used to simulate with associated variability the internal dosimetry in blood to both compounds during the rat DNT study, marking the animal POD.

13.1.1 Distribution and blood binding

For acibenzolar the V_{ss} applied in the minimal PBPK model was optimized based on the rat *in vivo* data after an IV dose (Punler and Tomlinson, 2017). For acibenzolar-acid K_p was predicted using the Method of Rodgers and Rowland (2007) and then V_{ss} predicted using Equation 13.1 (Sawada *et al.*, 1984).

$$V_{ss} = \sum V_t \cdot K_{p,t} + V_e \cdot E/P + V_p$$

Equation 13.1

Where V is the fractional body volume (L/kg) of a tissue (t), erythrocyte (e) or plasma (p) and E/P is the erythrocyte:plasma ratio.

The fraction unbound and blood to plasma ratio for acibenzolar and acibenzolar-acid were experimentally determined for female Wistar rats (Frost, 2017) and are shown in Section 8.2. A reliable *in vitro* measurement of blood to plasma ratio could not be obtained for acibenzolar and a default of 1 was used in the model and sensitivity analysis around this parameter was conducted.

13.1.2 Absorption

The oral absorption of acibenzolar was simulated using a first-order absorption model (Equation 4.1). k_a was obtained by fitting to the observed blood concentration data for acibenzolar-acid after oral dosing (1, 10 and 100 mg/kg acibenzolar) as acibenzolar was undetectable in blood at these doses. The fraction absorbed (f_a) was obtained from Molitor (1995) following oral doses of radiolabelled Acibenzolar at 1 mg/kg and 100 mg/kg.

13.1.3 Elimination

The hepatic, intestinal and plasma metabolism of acibenzolar input was derived from the *in vitro* experiments where the kinetic parameters (V_{max} and K_m) for the formation of acibenzolar-acid were estimated as described in Section 8.3.

The unbound intrinsic clearance in the liver was scaled from the *in vitro* V_{max} and K_m using Equation 13.2.

$$CLu_{int-H} = \frac{V_{max}}{K_m \cdot fu_{inc} + Cu_{Liv}} \cdot MPPGL \cdot LW \cdot 60/10^3$$

Equation 13.2

Where CLu_{int-H} (L/h) is the unbound intrinsic clearance in the liver, V_{max} (nmol/min/mg microsomal protein) and K_m (μ M) are the maximum rate of metabolism and Michaelis constant determined *in vitro*, respectively, Cu_{Liv} is the unbound concentration in the liver (Equation 4.2), fu_{inc} is the corresponding fraction unbound in the *in vitro* experiment, $MPPGL$ is the microsomal protein per gram of liver (mg/g) and LW is the liver weight (9 g). The term $60/10^3$ is for unit conversion.

Intestinal metabolism was incorporated into the PBPK model via the F_G term shown in equation 4.1 as detailed in the modelling and simulation companion report (Section 3.1 in Burt 2017).

The half-life of acibenzolar in plasma after IV dosing was optimized based on the rat *in vivo* data after an IV dose (Punler and Tomlinson, 2017) and for oral dose simulations the observed plasma half-life was not modified in order to simulate a worst-case scenario in terms of internal dosimetry.

Renal clearance of acibenzolar was not included in the model as this was found to be negligible at all of the doses administered in the rat PK study (Punler and Tomlinson, 2017).

In the acibenzolar-acid model, the hepatic metabolism of acibenzolar-acid was incorporated using an intrinsic clearance in rat hepatocytes and a corresponding fraction unbound in the incubation.

The observed *in vivo* renal clearance with respect to plasma after 1 mg/kg intravenous and oral doses was applied in the acibenzolar-acid model.

13.1.4 Rat PBPK Model Input Parameters

The final input model parameters and the source of the data are shown in Tables 7 and 8 with more details available in Section 3.1 of Burt (2017).

Table 7. Rat model input data for Acibenzolar

Physicochemical Parameters		
Parameter	Input	Source of Input
Molecular weight	210.3	
Log P	3.1	Experimental - Shake-flask method
Compound type	Neutral	
Blood Binding		
f_u	0.0469	Experimental - equilibrium dialysis
B/P ratio	1	Assumed, unable to be determined <i>in vitro</i> due to esterase metabolism.
Absorption – First-order Absorption Model		
ka 1 mg/kg PO dose	0.8 h⁻¹	Fitted to <i>in vivo</i> concentration-time data using the parameter estimation module in the Simcyp simulator.
ka 10 mg/kg PO dose	0.45 h⁻¹	
ka 100 mg/kg PO dose	0.2 h⁻¹	
fa	0.93	Absorption of radiolabeled material. Average of 0.5 and 100 mg/kg PO doses
$f_{u_{gut}}$	1	Assumed
Distribution – Minimal PBPK		
V_{ss} (L/kg)	15.29	Optimized <i>in vivo</i> IV concentration-time data in the parameter estimation module in Simcyp simulator.
Hepatic Metabolism		
V_{max} (nmol/min/mg protein)	519	Derived from experimental cryopreserved rat hepatocyte data
K_m (μ M)	69	
$f_{u_{inc}}$	0.919	Experimental - Cryopreserved rat hepatocyte data
Intestinal Metabolism		
V_{max} (nmol/min/mg protein)	134	Derived from experimental rat intestinal microsomal data
K_m (μ M)	117	
$f_{u_{inc}}$	0.877	Experimental - rat liver microsomal data
Plasma Metabolism		
IV dose half-life (min)	0.015	Optimized <i>in vivo</i> IV concentration-time data in the parameter estimation module in Simcyp simulator
PO dose half-life (min)	13.4	Derived from experimental rat plasma kinetics

Table 8. Rat model input data for acibenzolar-acid

Physicochemical Parameters		
Parameter	Input	Source of Input
Molecular weight	180.2	
Log P	2.24	Experimental - Shake-flask method
Compound type	Acid	
pKa	2.94	Experimental (OECD Method No. 112)
Blood binding		
f _u	0.0739	Experimental - equilibrium dialysis
B/P ratio	0.679	Experimental – <i>in vitro</i> blood and plasma concentrations
Distribution – Minimal PBPK		
V _{ss} (L/kg)	0.15	Predicted (Method 2 with the Simcyp simulator)
Hepatic Metabolism		
CL _{int} (μL/min/million cells)	0.596	Experimental - cryopreserved rat hepatocyte data
f _{uinc}	0.946	Experimental - cryopreserved rat hepatocyte data
Renal Clearance		
CL _R (mL/min)	2.1	Experimental – <i>in vivo</i> 1 mg/kg IV and PO doses

The rat models were used to simulate, with associated variability, the internal dosimetry to both acibenzolar and acibenzolar-acid compounds during the rat DNT study, marking the animal POD.

13.1.5 Incorporating Variability into Rat PBPK Model

As stated earlier the Simcyp Rat Simulator does not have variability included by default. However, the impact of variability of several parameters in the acibenzolar and acibenzolar-acid models were investigated by simulating oral doses of 1, 10 and 100 mg/kg acibenzolar using the R-Simcyp package (V1.5) developed for the R programming language. The R script used for this aspect of the study is supplied as part of the submission package and is detailed in Section 3.1.3 of Burt (2017).

The impact of variability in hepatic, intestinal and plasma esterase activity in the acibenzolar model and hepatic and renal clearance in the acibenzolar-acid model was investigated by Monte-Carlo simulation. All other parameters in both the acibenzolar and acibenzolar-acid models were maintained as used for simulations in rat without variability. For each simulation a population of 60 virtual rats (10 times the number of rats in the rat PK study) was created with the variable parameters randomly sampled assuming a log-normal distribution.

Overall, the simulated variability in acibenzolar-acid blood toxicokinetics was considered to reasonably describe the observed data (figure 8) where the population median concentration-time

profile is shown together with predicted variability covering the 5th to 95th percentiles. The parameters used to introduce variability were further examined to understand their contribution to the overall variability in terms of a sensitivity analysis.

Simulation of Oral Doses with Associated Variability

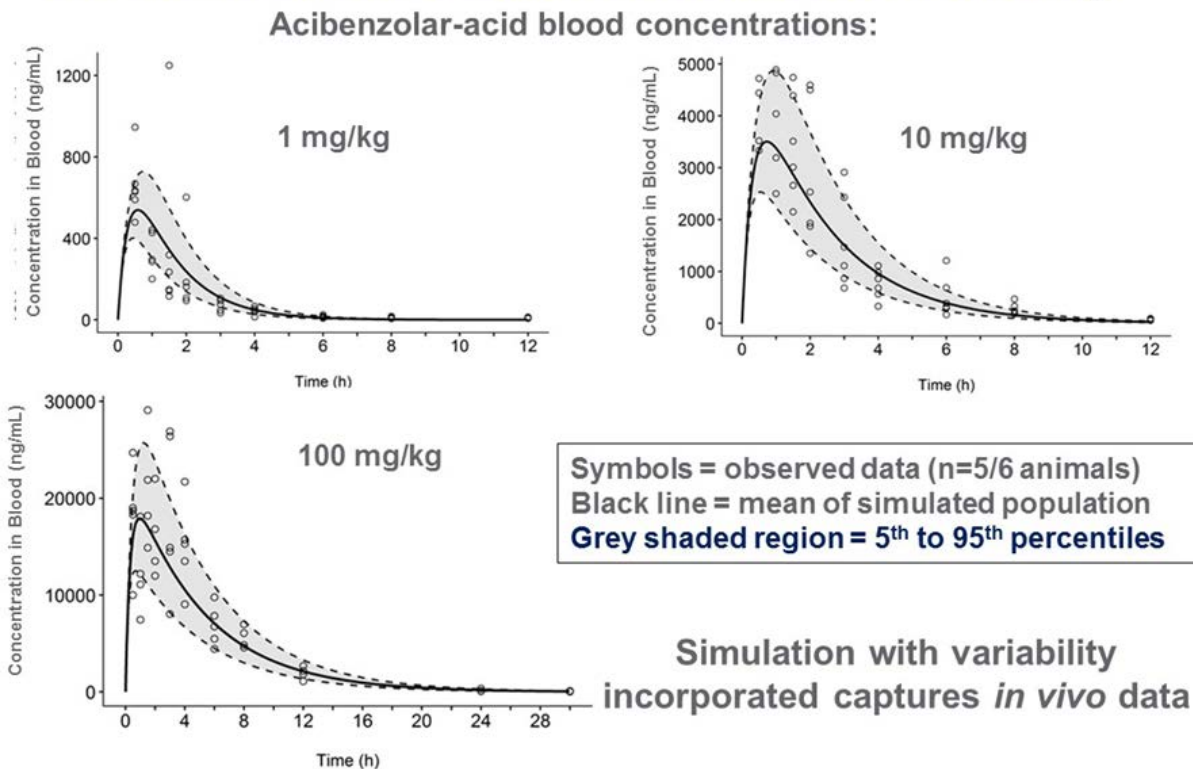


Figure 8: Simulated acibenzolar-acid blood concentration-time profiles with associated variability in rat following oral administration of acibenzolar at 1, 10 or 100 mg/kg.

13.1.6 Understanding Variability – Rat PBPK Model Sensitivity Analysis

After an oral dose of acibenzolar, the rapid and extensive conversion of acibenzolar to acibenzolar-acid during first-pass metabolism means that the simulated variability in acibenzolar-acid blood concentrations was almost entirely dependent on the variability in its renal clearance (the primary clearance pathway for acibenzolar-acid). This was apparent from simulations performed in the absence of variability in renal clearance in the acibenzolar-acid model. In this case the overall variability in simulated acibenzolar-acid blood concentrations was negligible (figure 9). More details can be found in Section 4.1.3 of Burt (2017).

Understanding Impact of Variability

The main impact of variability on acibenzolar-acid blood concentrations comes from renal clearance

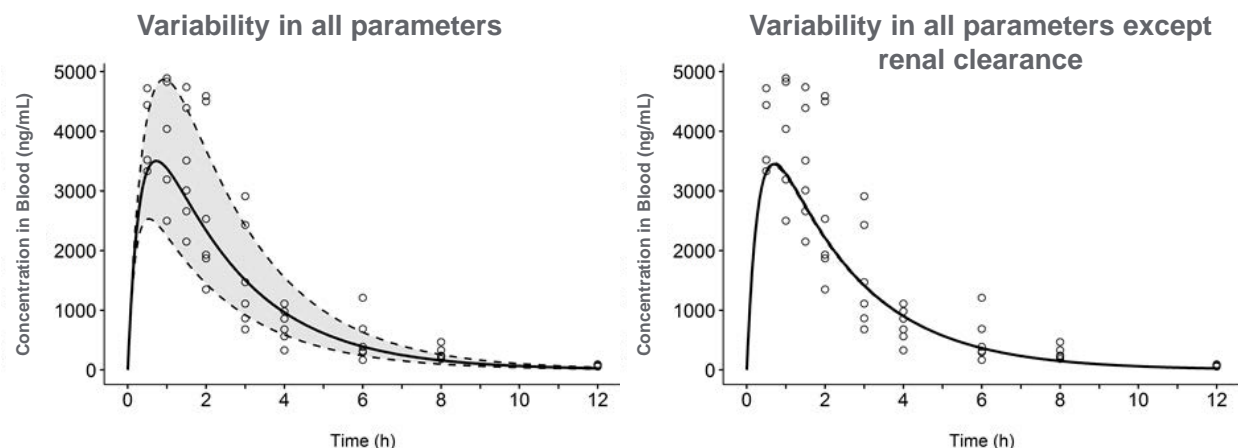


Figure 9: Simulated acibenzolar-acid blood concentration-time profiles with and without variability in renal clearance

In the simulations, a 30% CV was applied to renal clearance which is consistent with available literature data: Ochodnický et al (2009) defined glomerular filtration rate (GFR) in male Wistar rats ($n = 16$) of 0.53 ± 0.15 mL/min/100g (28% CV).

13.1.7 PBPK Model Acceptance

The PBPK models for acibenzolar and acibenzolar-acid were used to simulate the observed blood concentrations of both compounds after a 1 hour constant rate IV infusion at 1 mg/kg and, as shown above in figure 8, oral dosing at 1, 10 and 100 mg/kg in Female Wistar rats (Punler and Tomlinson, 2017). In this study acibenzolar was not detectable in blood after oral dosing.

The simulations were performed in 60 virtual rats (10 individual trials of 6 subjects each). For comparison and verification purposes the TK parameters (C_{max} , T_{max} , AUC and clearance) for acibenzolar-acid following an oral dose of 10 mg/kg (being close to the POD of 8.2 mg/kg) are shown in Table 9.

The descriptive statistics for the TK parameters in terms of geometric mean, CV%, 5th and 95th percentiles were similar but with the simulations tending to be slightly lower. However, the range in clearance, defined by the 5th to 95th percentiles, was captured by the simulations bringing confidence that the most important and sensitive parameter was well understood within the PBPK model.

Table 9. Observed and simulated summary TK parameters for acibenzolar-acid following an oral dose of 10 mg/kg acibenzolar with variability. Observed data represent data from 6 rats whereas the simulation was performed in 60 virtual rats (10 individual trials of 6 subjects each). All parameters are with respect to blood concentration. Geometric mean and CV are reported.

Parameter	Units	Observed ^a				Simulated ^a			
		Mean	CV (%)	Percentile		Mean	CV (%)	Percentile	
				5 th	95 th			5 th	95 th
AUC _(0,t)	ng.h/mL	13,165	28.2	9210	18075	10,617	25.6	7179	16453
C _{max}	ng/mL	4079	20.6	3359	4881	3470	20.0	2533	4871
CL	mL/h/kg	678	29.9	496	1004	751	25.6	484	1110
t _{max} ^b	h	0.5	-	0.5	1	0.7	-	0.49	1.08

^a = geometric mean

^b = median and range for t_{max}

With the model simulations reflecting the observed *in vivo* data and with a clear understanding of the associated variability in hand, the rat PBPK model was considered to be fit for purpose to meet the objective of predicting the internal dosimetry in the rat DNT study marking the POD used in this proof of concept. Obtaining this information would allow the derivation of the human equivalent dose and the interspecies DDEF (EF_{AK}) for use in risk assessments which utilize geometric mean data or that reflecting an ‘average individual’ (section 13.3.2, section 14).

It should also be noted that generation of variability within the human population is more comprehensive with virtual individuals being generated independently within Simcyp (section 4.3) and so was not influenced by the selective targeting of TK parameters used to introduce variability into the rat PBPK model.

13.1.8 Simulation of Dietary Administration and POD Study

As toxicokinetic data were not available for the rat DNT study used as the POD the acibenzolar-acid PBPK model was used to provide information on the internal dosimetry obtained during the study where acibenzolar was administered in the diet.

Administration of the POD acibenzolar dose of 8.2 mg/kg/day was simulated. The dose of acibenzolar was converted to an equivalent acibenzolar-acid dose based on the relative molecular weights of metabolite to parent and the acibenzolar fa (0.93). The resulting POD equivalent acibenzolar-acid dose was 6.53 mg/kg/day. The fraction of a total daily dose consumed in each 2 hour period was obtained from ‘TK Modeller’ version 1.0 software (McCoy et al 2012) which incorporates published data in rats (Yuan 1993; McCoy et al. 2012).

The resulting cumulative percentage of the acibenzolar dose absorbed via the diet of rats in each two hour period of a day in the rat DNT study is shown in Table 10. The R script used to do this is provided in the supplementary documentation.

Table 10. The cumulative percentage of the acibenzolar dose absorbed via the diet of rats in each two hour period of a day in the rat DNT study.

Hour of day	% acibenzolar absorbed
0	0.0
2	2.7
4	4.8
6	8.1
8	12.4
10	16.5
12	22.4
14	33.2
16	47.4
18	62.9
20	78.7
22	91.8
24	100.0

The absorption rate constant (k_a) for each two hour period was determined using equation 13.3. This was derived from the relationship between the oral dose of acibenzolar and its absorption rate constant (k_a) determined from the fitted oral *in vivo* data outlined in Section 13.1.2.

$$Acibenzolar\ k_a = 0.832 \times acibenzolar\ dose^{-0.301} \quad \text{Equation 13.3}$$

The acibenzolar-acid dose and acibenzolar absorption rate constants during each two hour period of the day of the DNT study were then used to simulate a series of constant rate iv infusions (figure 10) to mimic dietary input.

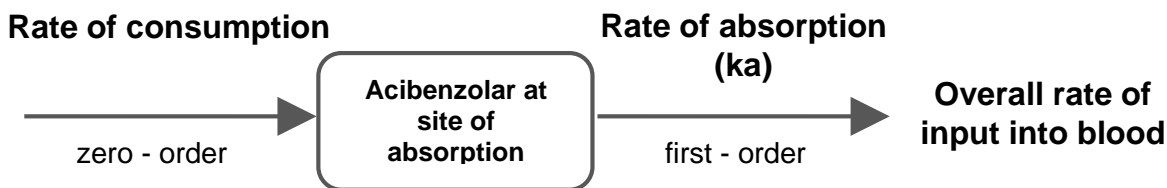


Figure 10: A schematic representation of the model used to define the overall rate of acibenzolar-acid input into blood for each two hour period of the DNT study.

Variability in the hepatic metabolism and renal clearance of acibenzolar-acid was included in the model and each simulation was performed in 10 virtual studies of 30 rats, leading to a total virtual population of 300 rats.

The TK of acibenzolar-acid were simulated over 14 days of dosing with the concentration-time profile in blood shown on the final day (figure 11) with $AUC_{(312,336)}$ used as the metric to define steady-state internal dosimetry in the study against which a human equivalent dose (HED) could be determined.

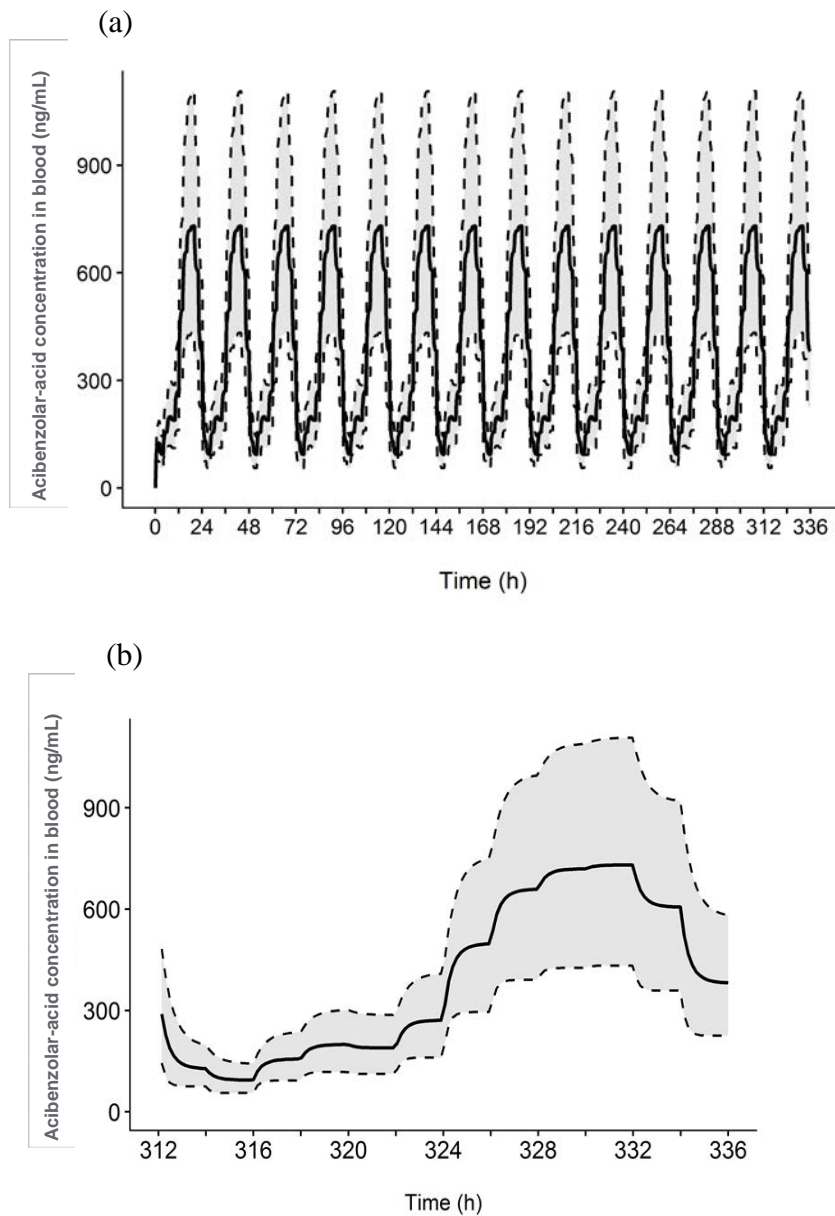


Figure 11: The simulated concentrations of acibenzolar-acid in blood following 14 days of administration of 8.2 mg/kg/day acibenzolar in the diet of rats during the DNT study. The solid black line is the mean of the simulated population ($n = 300$) and the dotted lines represent the 5th and 95th percentiles. 14 days (a) and on last day only (b).

The TK parameters obtained from the simulations together with geometric means and associated statistics, as appropriate, are shown in Table 11.

Table 11: Steady-state PK parameters for acibenzolar-acid after the simulated administration of 8.2 mg/kg/day acibenzolar in the diet of rats during the DNT study. The simulation was performed in 300 virtual rats (10 individual trials of 30 subjects). All parameters are with respect to blood concentration on day 14 of dosing.

Parameter	Units	Geomean	GeoSD	Minimum	Maximum
AUC _(312,336)	ng.h/mL	8866	1.33	4119	20887
C _{max}	ng/mL	702	1.33	326	1653
t _{max} ^a	h	332	-	331	332
CL	mL/h/kg	737	1.33	313	1587

^a median and range for tmax

13.2 Human PBPK Model

The corresponding human PBPK models were used to simulate the internal dosimetry of acibenzolar and acibenzolar-acid after acute and chronic dosing to healthy adults as well as to the potentially ‘at risk’ populations of children aged between 1 and 2 years and adults with moderate and severe renal impairment. A summary of the final input parameters is shown in Tables 12 and 13 with more details available in Section 3.3 of Burt 2017. For input into Simcyp, the parameters (e.g., half life, renal clearance) are required to be with respect to plasma. The output parameters are all reported with respect to blood having been corrected for blood to plasma ratio within the simulator.

Full details of the building, refinement and the final inputs and outputs of the human PBPK model can be found in the companion report (Burt, 2017). The key points are summarized below.

13.2.1 Distribution and Blood Binding

For Acibenzolar *in vivo* V_{ss} was scaled from the rat using single species allometry with an exponent of 1. Given the negligible difference between rat and human, fu was not incorporated into this scaling approach.

For acibenzolar-acid, V_{ss} was predicted using the method of Rodgers and Rowland (Rodgers and Rowland, 2007). Variability in the prediction of V_{ss} was introduced via incorporating inter-individual variability in the tissue compositions used to predict K_p and the volume and E/P terms in Equation 13.1.

The fraction unbound and blood to plasma ratio for acibenzolar and acibenzolar-acid were experimentally determined in human matrices (Frost, 2017). However, a reliable *in vitro* measurement of blood to plasma ratio could not be obtained for acibenzolar due to poor recovery in the assay, most likely due to esterase metabolism in erythrocytes. Therefore, the blood to plasma ratio for acibenzolar was predicted from log P, pKa and fu, using the B/P prediction method incorporated into the Simulator (Turner et al., 2011).

13.2.2 Absorption

The fraction of acibenzolar absorbed after an oral dose in the human model was assumed to be the same as observed in rats (0.93). In the absence of a human measurement it is acknowledged there is significant uncertainty in this estimate. However, as near complete absorption was observed in rat, human absorption is unable to be significantly higher and hence this assumption brings conservatism into the predictions by representing a near worst-case scenario in terms of human internal dosimetry.

The rate of oral absorption was calculated based on the relationship between k_a and dose defined in the rat oral dose simulations (Equation 13.3) followed by allometric extrapolation.

Allometric extrapolation of the dose specific k_a was performed using an exponent of -0.25 (Equation 13.4) as is typically the case for first-order rate constants.

$$k_{a_{human}} = k_{a_{rat}} \cdot \left(\frac{BW_{human}}{BW_{rat}} \right)^{-0.25}$$

Equation 13.4

For healthy adults, the body weight of a Population Representative for the Simcyp healthy volunteer population was applied (80.7 kg) whereas for children, the average body weight of 1000 simulated individuals aged between 1 and 2 years using the Simcyp paediatric population was applied (12 kg). A typical body weight of 0.25 kg was applied for the rat.

13.2.3 Elimination

The hepatic, intestinal and plasma metabolism of acibenzolar was defined from the experiments whereby V_{max} and K_m for the formation of acibenzolar-acid were estimated (appendix 1 of Burt, 2017).

CLu_{int-H} and F_G were scaled from *in vitro* metabolism data using the same equations as for rats, applied within the human Simulator (Equation 13.2 and Equation 4.1, respectively). Inter-individual variability was incorporated into the scaling factors applied in these equations (Rostami-Hodjegan and Tucker, 2007).

For the purposes of applying ontogeny in paediatric simulations all hepatic metabolism of acibenzolar was assumed to be mediated by CES1 and intestinal metabolism was assumed to be mediated by CES2.

In order for the observed V_{max} in cryopreserved hepatocytes to be incorporated into the human PBPK model as hepatic CES1 it was converted to an equivalent microsomal V_{max} using Equation 8.1 and Simcyp North European Caucasian population means of 117.5 million cells/g liver and 39.8 mg protein/g liver for HPGL and MPPGL, respectively.

In a similar manner to rat intestinal microsomes, the human intestinal microsomal V_{max} was scaled to a whole cell (enterocyte) V_{max} using Equation 8.2 with Simcyp North European Caucasian population means of 117.5 million cells/g liver and 39.8 mg protein/g liver for HPGL and MPPGL, respectively.

In human intestinal microsomes a corresponding fraction unbound in the incubation of 0.944 was experimentally determined at a protein concentration of 0.001 mg/mL (Frost, 2017). As the protein concentration in the kinetics experiment in human intestinal microsomes was significantly higher (0.05 mg/mL) the experimental fu was converted to reflect this increase in protein concentration using Equation 13.5.

$$fu_{inc2} = \frac{1}{\frac{P_2}{P_1} \cdot \left(\frac{1 - fu_{inc1}}{fu_{inc1}} \right) + 1}$$

Equation 13.5

Where fu_{inc1} and fu_{inc2} represent the measured and converted fraction unbound in the incubation, respectively and P_1 and P_2 represent the protein concentration for the measured and converted fu_{inc} , respectively.

A half-life of acibenzolar in plasma of was defined based on the intrinsic clearance in human plasma (V_{max}/K_m) and the volume of plasma in the experiment (0.2 mL) using Equation 13.6.

$$half - life = \frac{\ln(2) \cdot V}{CL_{int}}$$

Equation 13.6

The metabolism of acibenzolar-acid in cryopreserved hepatocytes was negligible (Frost, 2017).

The acibenzolar-acid rat renal clearance of 2.1 mL/min determined following intravenous and oral administration was scaled using single species allometry without correction for fu (Equation 13.7). as this method was found to perform well when compared to several others in a meta-analysis previously performed at Simcyp (Burt et al., 2012).

$$CL_{R,human} = CL_{R,rat} \cdot \left(\frac{BW_{human}}{BW_{rat}} \right)^{0.75}$$

Equation 13.7

The body weight of a Population Representative for the Simcyp healthy volunteer population (80.7 kg) was applied alongside a rat body weight of 0.25 kg.

13.2.4 Human PBPK Model Input Parameters

The final human parameters incorporated into the model and the source of the data are summarized below in Tables 12 and 13.

Table 12. Human model input data for Acibenzolar

Physicochemical Parameters		
Parameter	Input	Source of Input
Molecular weight	210.3	
Log P	3.1	Experimental - Shake-flask method
Compound type	Neutral	
Blood binding		
fu	0.0523	Experimental Equilibrium dialysis
B/P ratio	0.877	Predicted - (QSAR model in Simcyp simulator)
Absorption – First-order absorption model		
fa	0.93	Assumed equivalent to rat
fu _{gut}	1	Assumed
Distribution – Minimal PBPK Model		
V _{ss} (L/kg)	15.29	Allometric scaling of rat V _{ss} (exponent of 1)
Hepatic Metabolism (CES1)		
V _{max} (nmol/min/mg protein)	1473	Derived from Experimental Cryopreserved human hepatocyte data
K _m (μM)	92	
fu _{inc}	0.982	Experimental - Cryopreserved human hepatocyte data
Intestinal metabolism (CES2)		
V _{max} (nmol/min/mg protein)	38	Derived from experimental human intestinal microsomal data
K _m (μM)	311	
fu _{inc}	0.252	Converted from experimental human liver microsome data accounting for protein concentration
Plasma metabolism		
half-life (min)	252	Experimental human plasma data

Table 13. Human model input data for Acibenzolar-acid

Physicochemical Parameters		
Parameter	Input	Source of Input
Molecular weight	180.2	
Log P	2.24	Experimental - shake-flask method
Compound type	Acid	
pKa	2.94	Experimental (OECD Method No. 112)
Blood binding		
fu	0.0206	Experimental - equilibrium dialysis
B/P ratio	0.651	Experimental – <i>in vitro</i> blood & plasma concentrations
Distribution – minimal PBPK		
V _{ss} (L/kg)	0.10	Predicted (Using Method 2 in Simcyp simulator)
Renal Clearance		
CL _R (L/h)	9.60	Scaled rat CL _R using allometry

13.2.5 Human PBPK Model Sensitivity Analysis

Sensitivity of simulated acibenzolar and acibenzolar-acid blood concentrations to parameter uncertainty was investigated. The impact of uncertainty in several parameters in the human acibenzolar and acibenzolar-acid models was assessed via sensitivity analysis using an acute dose scenario in healthy adults. A summary is given below but further details can be found in Section 4.6 of Burt (2017).

Sensitivity analysis performed on the absorption rate constant (model default: 0.45 h⁻¹, range: 0.045 to 4.5 h⁻¹) and blood to plasma ratio (model default: 0.877, range: 0.55 to 8.77) in the acibenzolar model revealed negligible change in the simulated AUC_{0,24} for acibenzolar or acibenzolar-acid in blood across the ranges investigated.

The blood AUC_{0,24} of acibenzolar but not acibenzolar-acid was sensitive to changes in the plasma half-life applied in the acibenzolar model (model default: 252 h, range: 0.02 to 252 h). In this case the blood AUC_{0,24} of acibenzolar decreased significantly as the plasma half-life was decreased but a plateau was reached close to the model default. The blood AUC_{0,24} of acibenzolar-acid was sensitive to changes in renal clearance (model default: 9.6 L/h, range: 0.96 to 96 L/h) applied in the acibenzolar-acid model, particularly as it was decreased.

With this analysis complete and in view of its intended use the human PBPK model was considered fit for purpose to allow simulation of human internal dosimetry scenarios in the intended populations.

13.3 Dose Proportionality, Human Equivalent Dose Derivation and Simulation of Internal Dosimetry at the POD

13.3.1 Dose Proportionality

To examine dose proportionality within the human PBPK model a typical adult individual was selected and acibenzolar-acid AUC was obtained via simulation of chronic doses ranging from 0.00015 mg/kg/day to 150 mg/kg/day (section 4.3.6 of Burt, 2017).

A linear equation was found to be a good fit to the simulated acibenzolar-acid AUCs (figure 12) and was used to obtain a human equivalent dose of acibenzolar matching the simulated geometric mean of acibenzolar-acid AUC in the rat DNT study.

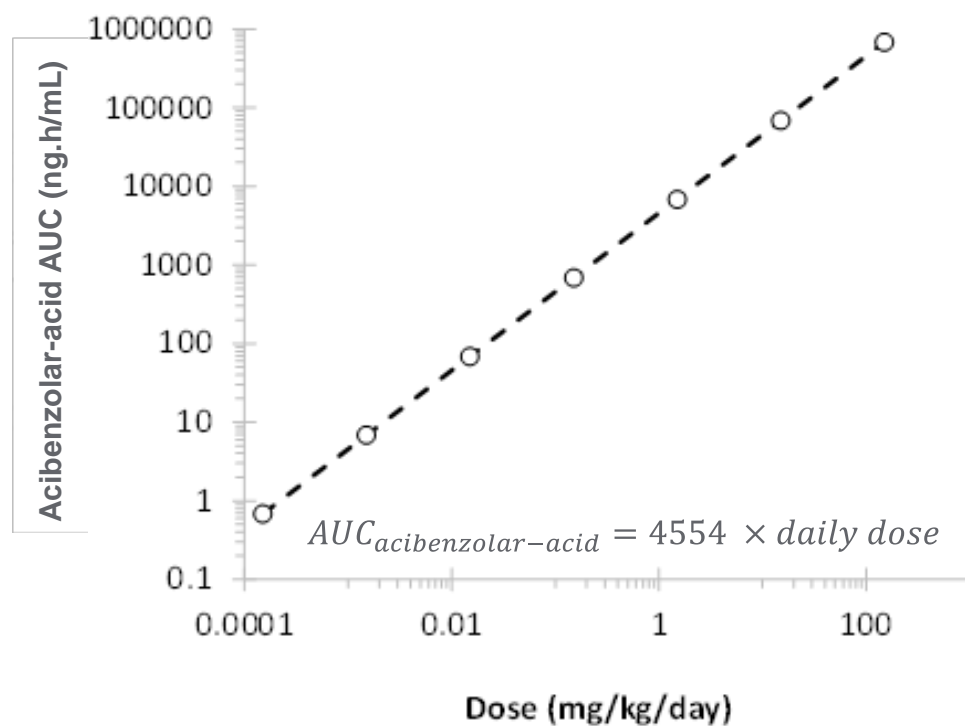


Figure 12: The simulated geometric mean acibenzolar-acid $AUC_{(144,168)}$ in blood after simulated chronic oral doses of 0.00015 to 150 mg/kg/day acibenzolar in healthy adults ($n = 1000$). The dashed line represents a linear fit to the data.

13.3.2 Human Equivalent Dose

The rat geometric mean blood AUC of the acibenzolar-acid following simulation of the POD dose of 8.2 mg/kg/day obtained in the rat DNT study was 8866 ng.h/mL (Table 9) resulting in a HED of acibenzolar of 1.947 mg/kg (or 0.649 mg/dose if simulating a chronic scenario) and could be employed in the calculation of an interspecies DDEF such as EF_{AK} . Further details of derivation of the HED can be found in Section 4.3.6 of Burt (2017).

13.3.3 Simulation of Human Internal Dosimetry at the HED

The internal dosimetry of 1000 adult individuals (10 trials of 100 individuals per trial) was simulated at the HED to provide a reference point based upon area under the curve (AUC) from which to determine the ‘toxicokinetic safety margin’ from simulations of consumer exposures. The TK parameters and descriptive statistics from these simulations are given in Table 14. Further details can be found in Section 4.3.6 of Burt (2017).

Table 14: Summary TK parameters for acibenzolar-acid after simulated chronic human equivalent dose (1.947 mg/kg). The simulations were performed in 1000 virtual individuals (10 trials of 10 subjects in each trial). All parameters are with respect to blood concentration.

Parameter	Units	Geomean	GeoSD	Minimum	Maximum
AUC _(312,336)	ng.h/mL	8875	1.47	2690	37783
C _{max}	ng/mL	1961	1.47	766	4196
t _{max} ^a	h	154	-	144	155
CL	mL/h/kg	175	1.47	41.0	577

^a median and range for t_{max}

13.4 Simcyp Human Population Libraries and Simulation Scenarios

The different human populations defined within the Simcyp simulator and the simulations carried out in each population are described below.

The TK of acibenzolar and acibenzolar-acid were simulated using the Simcyp North European Caucasian (adult) and pediatric population libraries following acute and chronic dosing of acibenzolar at doses based on residue trial and consumer consumption data (Table 6).

A specific North American population is not available. However, considering that the ethnic mix in Europe and North America is similar it would be expected the population files would be similar. Therefore, for a proof of concept study, the North European Caucasian population was deemed to be adequate.

The default Simcyp parameters for creating a virtual North European Caucasian population (physiological parameters including liver volume and blood flows, enzyme abundances etc.) have been described previously (Howgate *et al* 2006).

The Simcyp Pediatric population accounts for changes to physiological parameters during development from neonates to adolescence (Johnson and Rostami-Hodjegan 2011, Salem *et al.*, 2013). This includes the ontogeny of hepatic CES1 and intestinal CES2 enzyme abundance which develop mainly in the first 2 years of life (Yang *et al* 2009; Zhu *et al* 2009; Shi *et al* 2011; Chen *et al* 2015).

In acute dose simulations a single oral dose of acibenzolar was administered to 1000 virtual individuals (10 trials of 100 individuals) aged between either 18 and 95 years (adult simulations)

or 1 and 2 years (children simulations), with 50% of the population being female to be reflective of the general population.

In chronic dose simulations acibenzolar was dosed three times a day for 7 days (7 am, 12 pm and 5 pm, corresponding with theoretical meal times) with the same population demographics as for acute dosing. The pharmacokinetics of acibenzolar and acibenzolar-acid were at steady-state by the final day of dosing.

Similarly, the pharmacokinetics of acibenzolar and acibenzolar-acid were simulated in the moderate ($\text{GFR} = 30 - 60 \text{ mL/min}$) and severe ($\text{GFR} = < 30 \text{ mL/min}$) adult renal impairment population libraries of the Simcyp Simulator (Rowland Yeo, Aarabi *et al.* 2011). The adult acute and chronic doses were again as described in Section 11 and simulations in 1000 virtual individuals (10 trials of 100 individuals) aged between 20 and 85 years, with 50% of the population being female.

Further details of the simulations can be found in Section 4.3 of Burt (2017). The output files of all the simulations are listed in appendix 2 and are also available as supporting documentation.

13.5 Simulations of Consumer Exposure Scenarios in Adults, Children (1 – 2 years) and Renally Impaired Populations

The simulated blood concentration-time profiles in each population were similar in shape and only differed in the amount of acibenzolar and acibenzolar-acid present reflective of the differences in clearance. With the chronic dosing scenario mimicking daily dosing concurrent with 3 meals per day even in the population with the lowest clearance (severe renally impaired) there was no evidence of significant accumulation at the end of each day.

Examples of the simulated acibenzolar–acid blood concentration-time profiles following acute and chronic exposure scenarios in healthy adult humans are shown in figure 13. The blood concentrations of acibenzolar-acid following (a) a single acute oral dose of 0.002825 mg/kg, (b) chronic oral dosing of 0.000157 mg/kg/day (split into 3 equal doses per day) for 7 days and (c) on the final day of dosing is shown.

Similarly, examples of the simulated acibenzolar–acid blood concentration-time profiles following acute and chronic exposure scenarios in the severe renal impairment population are shown in figure 14 following (a) a single acute oral dose of 0.002825 mg/kg and (b) on the final day of chronic oral dosing of 0.000157 mg/kg/day (split into 3 equal doses per day) for 7 days.

The corresponding TK parameters and descriptive statistics for the acute and chronic scenarios in each of the human populations is given in Table 15.

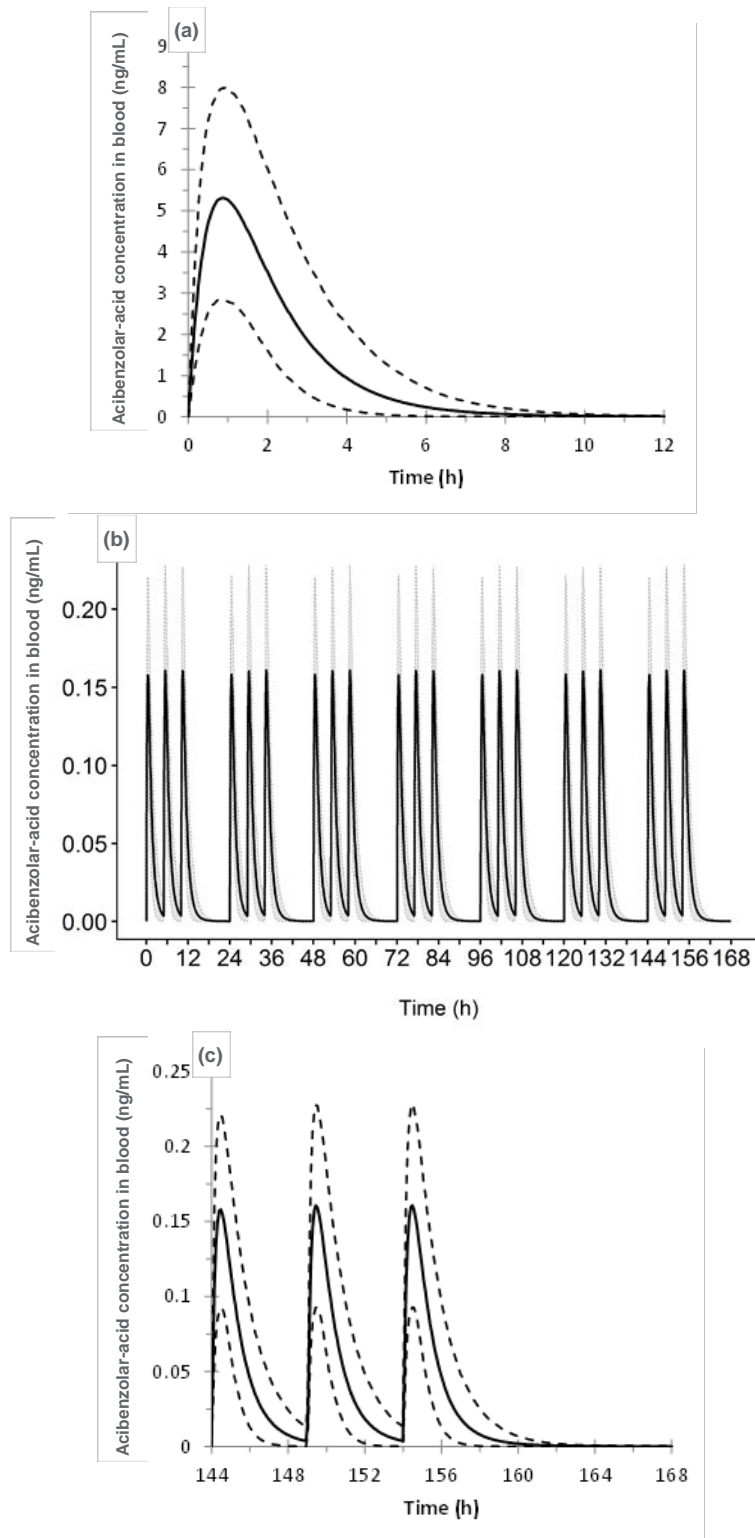


Figure 13: The simulated blood concentrations of acibenzolar-acid in healthy adult humans following (a) acute oral dosing of 0.002825 mg/kg, (b) chronic oral dosing of 0.000157 mg/kg/day acibenzolar in (for 7 days) and (c) on the final day of dosing. The solid black line is the mean of the simulated population ($n = 1000$) and the dotted lines represent the 5th and 95th percentiles.

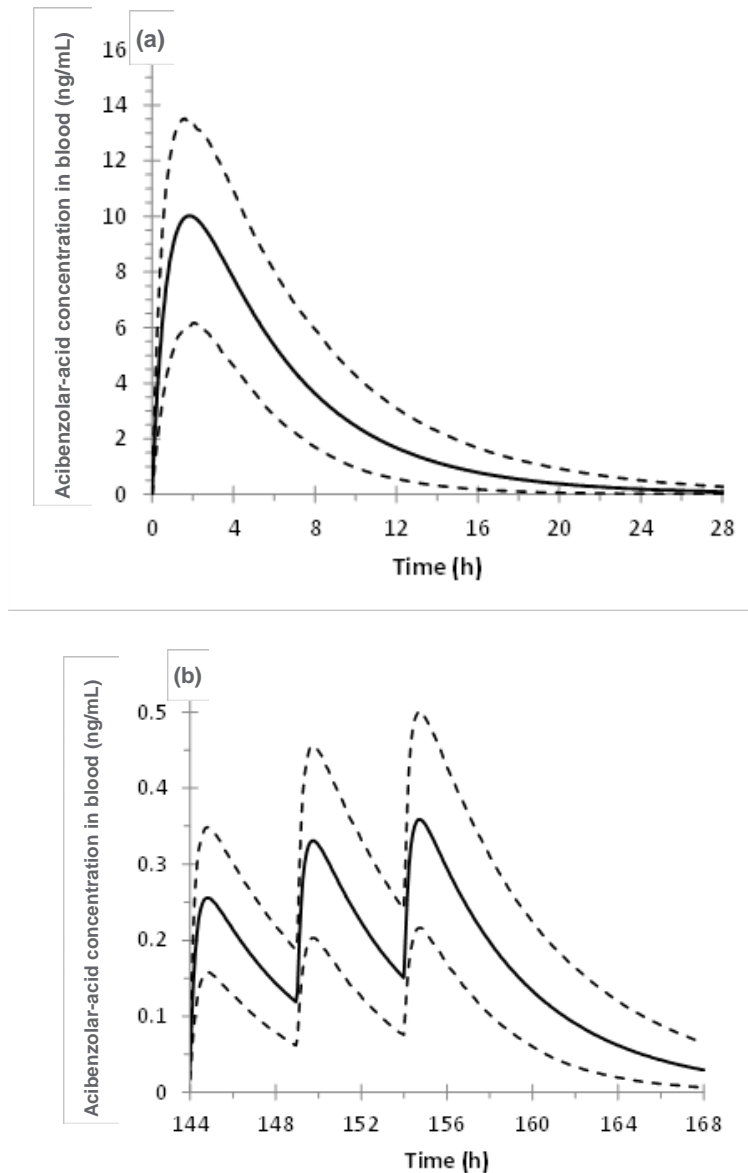


Figure 14: The simulated blood concentrations of acibenzolar-acid in severe renally impaired adult humans following (a) acute oral dosing of 0.002825 mg/kg and (b) on the final day of chronic oral dosing of 0.000157 mg/kg/day acibenzolar (for 7 days). The solid black line is the mean of the simulated population (n = 1000) and the dotted lines represent the 5th and 95th percentiles.

The 'toxicokinetic safety margins' as defined by the relative AUC with respect to that obtained in the adult population when dosed with the HED and expressed as the lowest AUC at the HED divided by and the highest AUC obtained in each human exposure scenario are given in Table 16.

Table 15: Summary TK parameters in blood for acibenzolar-acid after simulated oral acute and chronic dose scenarios of acibenzolar exposure in adults, children 1 – 2 years and renally impaired human populations.

Population	Dosing Regimen	AUC (ng.h/mL)		Clearance (mL/h/kg)	
		Geomean	95 th Percentile	Geomean	5 th Percentile
Adult	Acute	12.9	24.0	175	93.9
	Chronic	0.72	1.33	175	94.0
Children 1 – 2 years	Acute	6.72	12.1	335	186
	Chronic	0.37	0.67	339	187
Moderate Renal Impairment	Acute	32.8	51.3	68.6	43.9
	Chronic	1.82	2.85	68.7	43.9
Severe Renal Impairment	Acute	71.3	112	31.6	20.0
	Chronic	3.96	6.23	31.6	20.1

Simulations were performed in 1000 virtual individuals (10 trials of 100 subjects in each trial) with an acute dose of 0.002825 mg/kg and a chronic dose of 0.000157 mg/kg. All parameters are with respect to blood concentration. Geomean and 95th percentile (AUC) and 5th percentile (CL) are presented to allow calculation of DDEFs (*i.e.* EF_{HK}).

Table 16: Internal dosimetry, as defined by AUC, and multiples of AUC to acibenzolar-acid in blood after simulated oral acute and chronic consumer exposure to acibenzolar in adults, children 1 – 2 years and renally impaired human populations. The simulation was performed in 1000 virtual individuals (10 trials of 10 subjects in each trial).

Population	Dosing Regimen	Dose (mg/kg)	AUC (ng.h/mL)		Multiples of AUC*
			Geomean	Maximum	
Adult	Acute	0.0002825	12.9	54.8	49
	Chronic	0.000157	0.72	3.05	883
Children 1 – 2 years	Acute	0.005303	12.6	33.1	81
	Chronic	0.000978	2.31	6.10	441
Moderate Renal Impairment	Acute	0.0002825	32.8	63.6	42
	Chronic	0.000157	1.82	3.53	762
Severe Renal Impairment	Acute	0.0002825	71.3	140	19
	Chronic	0.000157	3.96	7.75	347

* **Toxicokinetic Safety Margin** determined by comparing the maximum simulated AUC following each consumer exposure scenario with the minimum AUC simulated for the healthy adult population at the human equivalent dose (Table 8, minimum AUC = 2690 ng.h/mL).

In line with the simulations and the observed data in rat, the simulated acibenzolar concentrations in blood after oral dosing in humans were negligible (less than 0.002 ng/mL in all scenarios). After acute dosing the mean acibenzolar-acid AUC_{0,24} in children aged between 1 to 2 years was within 3% of the corresponding AUC_{0,24} in adults (aged 18 – 95 years). However, due to an increase in the chronic dose for children, the mean acibenzolar-acid AUC_{144,168} was 3.2 fold higher in children compared to adults. For both acute and chronic dosing scenarios, the mean simulated acibenzolar-acid blood AUCs in moderate and severe renal impairment were 2.4-fold and 5.2-fold higher, respectively, than those in the corresponding healthy adults.

14 Application of Population based PBPK Models to Obtain Toxicokinetic Data Derived Extrapolation Factors and Toxicokinetic Composite Factors

14.1 Toxicokinetic Data Derived Extrapolation Factors EF_{AK} & EF_{HK}

14.1.1 Selection of Dose Metric

TK ratios for either interspecies or intraspecies extrapolation should be informed by the mode of action to select the relevant dose metric such as AUC or C_{max} . Clearance (CL) can also be used when the relevant dose metric is AUC or concentration at steady-state.

A reasonable assumption is that any effects resulting from sub-chronic or chronic exposure would normally be related to AUC rather than C_{max} . In cases where the data are not sufficient to make a clear decision then the AUC or CL should be used as this would be health protective because there is likely to be greater variability in human AUC and CL than in C_{max} .

In the database of acibenzolar toxicity endpoints and POD (Appendix 1) there is no indication that acibenzolar has any effects attributable to a single acute oral exposure and the 8.2 mg/kg/day used in this white paper as the POD was taken from a repeat dose dietary study where it was shown that steady-state was reached in the simulations. Therefore, for the purpose of this proof of concept, in the absence of tissue specific data it is assumed that steady-state systemic blood concentrations are representative of the tissue concentrations.

Taking into account the above assumptions to demonstrate application of our model-derived toxicokinetic DDEFs CL was chosen as the internal dose metric. In addition, in view of there being dose proportionality, as a dose-independent parameter CL would allow a single TK ratio to be defined for each population when different doses were examined within the same population such as acute and chronic scenarios.

This is also justified by considering that acibenzolar-acid is a renally cleared compound, being the mechanism by which it is cleared from the body, and is the most sensitive parameter in the PBPK model influencing variability in the internal dosimetry.

14.1.2 Human Equivalent Dose and Animal to Human Interspecies Toxicokinetic Extrapolation Factor, EF_{AK}

When animal and human data are available, EF_{AK} (the interspecies extrapolation factor) is derived using a ratio of external or applied doses producing the same AUC or a ratio of dose-independent clearance.

As previously described human equivalent dose (HED) is the human external dose that leads to the same dose metric as the external dose in test animals at the POD. HED was based upon internal dosimetry expressed as AUC and obtained from an examination of human dose

proportionality in a typical individual (section 13.3.1). The animal POD was based on an administered dose of 8.2 mg/kg/day in the rat DNT study. The human equivalent dose in the healthy adult population was 1.947 mg/kg (section 13.3.2). Taking into account the relationship between dose, AUC and clearance EF_{AK} can be calculated as:

$$EF_{AK} = \frac{Animal\ POD}{HED} = \frac{CL_{animal}}{CL_{human}}$$

and gives a model based data derived EF_{AK} for acibenzolar-acid of 4.22 that can be employed in a risk assessment.

14.1.3 Defining Interindividual Variability in Human Populations - Intraspecies Toxicokinetic Extrapolation Factor, EF_{HK}

EF_{HK} is a comparison of dose metrics resulting from the same external dose across the human population(s). EF_{HK} is the ratio of the dose metric at a percentile of the distribution intended to represent the sensitive or ‘at risk’ population and the dose metric at a central-tendency measure of the general or the entire population. For this proof of concept, the sensitive populations are defined separately rather than as a subset of the general population.

Therefore, using the data obtained from our simulations of the human populations EF_{HK} could be calculated as:

$$EF_{HK} = \frac{AUC_{sensitive}}{AUC_{general}} \text{ OR } \frac{Cmax_{sensitive}}{Cmax_{general}} \text{ OR } \frac{CL_{general}}{CL_{sensitive}}$$

As outlined above (section 14.1.1) clearance of acibenzolar-acid was chosen as the metric against which to define the intraspecies toxicokinetic extrapolation factor (EF_{HK}) for the specific human populations targeted in this investigation. Although the doses were different for the acute and chronic scenarios the same individuals in each population were used and so use of clearance allowed these differences in dose to be taken into account and provide an EF_{HK} for each human sub-population.

EF_{HK} was calculated using the geometric mean in the adult population (175 mL/h/kg, Table 14) as representative of the general population divided by the 5th percentile clearance of the targeted ‘sensitive’ or ‘at risk’ populations (i.e. children and renally impaired). The EF_{HK} for each population is shown in Table 17 and are available for use in a risk assessment to cover each human population.

Table 17: The 5th percentile clearance obtained following simulation of 1000 individuals in each human population and used to derive the intraspecies extrapolation factor EF_{HK}

Population	Clearance (mL/h/kg) 5 th Percentile	EF_{HK} ¹
Adult	94	1.86
Children 1 – 2 years	186	0.94
Moderate Renal Impairment	44	3.97
Severe Renal Impairment	20	8.71

¹Clearance geomean from the healthy adult population of 175 mL/h/kg used as the reference point for the general population for calculation of EF_{HK} .

Note: EF_{HK} based upon clearance using the 2.5th percentile and 1st percentile of the various populations as well as EF_{HK} based upon C_{max} and AUC using 95th, 97.5 and 99th percentiles determined following simulations for each population at the same dose can be made available if deemed necessary to carry out more conservative or alternative risk assessments using a different dose metric.

14.2 Toxicokinetic Composite Factors

The data derived toxicokinetic composite factor (CF_{TK}) for use in a risk assessment is simply obtained by multiplying EF_{AK} and EF_{HK} as shown below.

$$CF_{TK} = EF_{AK} \times EF_{HK}$$

The toxicokinetic composite adjustment factors for each human population using clearance as the dose metric is given in Table 18.

Table 18: Toxicokinetic Composite Factor (CF_{TK}) for the targeted human populations using clearance as the dose metric.

Population	EF_{AK}	EF_{HK}	CF_{TK}
Adult	4.22	1.86	7.9
Children 1 – 2 years	4.22	0.94	4.0
Moderate Renal Impairment	4.22	3.98	16.8
Severe Renal Impairment	4.22	8.71	36.8

15 Composite Factors for Risk Assessment

The overall composite factor (CF) for use in risk assessment is obtained by combining extrapolation factors to take into account inter and intraspecies differences in both toxicokinetics and toxicodynamics (section 3) and is calculated as shown below.

$$CF = EF_{AK} \times EF_{AD} \times EF_{HK} \times EF_{HD}$$

We have outlined the derivation of a CF_{TK} to account for the data derived toxicokinetic extrapolation factors EF_{AK} and EF_{HK} .

However, as also stated in section 3 the approach detailed in this submission proposes methodology to address toxicokinetic uncertainty only and toxicodynamic uncertainty is not addressed.

Therefore, for risk assessment purposes, in the absence of specific toxicodynamic data, default uncertainty factors are employed to take into account toxicodynamic differences and is termed TD_{UF} .

$$TD_{UF} = AD_{UF} \times HD_{UF}$$

Where AD_{UF} is the intraspecies (animal to human) toxicodynamic uncertainty factor and HD_{UF} is the intraspecies (human) toxicodynamic uncertainty factor.

For this proof of concept taking the subdivision of toxicokinetics and toxicodynamics as used by the US EPA the default AD_{UF} is 3.16 and the default HD_{UF} is 3.16 giving a combined UF_{TD} of 10. The overall CF for risk assessment then becomes a combination of CF_{TK} and TD_{UF} as shown below.

$$CF = CF_{TK} \times TD_{UF}$$

Table 19 shows the data derived toxicokinetic extrapolation factors and toxicodynamic uncertainty factor together with the corresponding composite factors that could be applied to a human risk assessment for each targeted population.

Table 19: Toxicokinetic extrapolation, toxicodynamic uncertainty factors and Composite Factors for each population available for use in human risk Assessments.

Population	EF_{AK}	EF_{HK}	CF_{TK}^1	TD_{UF}	CF^2
Adult	4.22	1.86	7.9	10	79
Children (1 – 2 years)	4.22	0.94	4.0	10	40
Moderate Renal impairment	4.22	3.98	16.8	10	168
Severe Renal Impairment	4.22	8.71	36.8	10	368

¹ calculated as $CF_{TK} = EF_{AK} \times EF_{HK}$

² calculated as $CF = CF_{TK} \times TD_{UF}$

It should also be noted that additional factors dictated by policy may be applied as required to the CF, for example the Food Quality and Protection Act Factor (FQPA) in the U.S. or the Pest Control Products Act (PCPA) factor in Canada.

16 Acibenzolar Example Risk Assessment Employing Toxicokinetic DDEFs

The acute and chronic reference doses used for conducting dietary risk assessments are calculated by dividing the animal dose representing the POD by the composite factor (CF).

$$Reference\ Dose = \frac{POD_{Animal}}{CF}$$

Dietary exposures have been calculated based on the information summarized in Section 10. The acute dietary (food and drinking water) exposure assessment was a refined Tier III assessment; therefore, the combined food and drinking water exposures at the 99.9th percentile were reported for each population subgroup and are shown below as dietary exposure in mg/kg/day (Table 20). Dietary intake of renally impaired individuals were not distinguished in the (NHANES) consumption database and in this work it was conservatively assumed that individuals with renal impairment consume the same diet as healthy adults.

The risk assessment was conducted by comparing the reference dose to the dietary exposure for each population subgroup (% Reference Dose). Dietary exposure below the reference dose is not likely to be associated with adverse health risks and is generally considered to be of no concern.

Table 20: Summary of example acibenzolar human risk assessment for each population giving composite factors, reference dose, dietary exposure and percent of reference dose met by dietary exposure

Population	Scenario	CF	Reference Dose (mg/kg) ¹	Dietary Exposure (mg/kg/day)	% of Reference Dose
Adult	Acute	79	0.104	0.002825	2.7
	Chronic	79	0.104	0.000157	0.2
Children 1 – 2 years	Acute	40	0.205	0.005303	2.6
	Chronic	40	0.205	0.000978	0.5
Moderate Renal Impairment	Acute	168	0.049	0.002825	5.8
	Chronic	168	0.049	0.000157	0.3
Severe Renal Impairment	Acute	368	0.022	0.002825	12.8
	Chronic	368	0.022	0.000157	0.7

¹ Reference Dose = POD_{Animal}/CF , $POD_{Animal} = 8.2 \text{ mg/kg}$

The acute and chronic dietary risks for acibenzolar do not exceed the level of concern (% of reference dose < 100 percent) for all population subgroups, as shown in Table 20. One advantage of the population based PBPK modelling approach is the ability to quickly identify and evaluate potentially sensitive populations including those with different consumption patterns such as children or those with disease states such as renal impairment.

17 Application of Human PBPK Model to Indicate Toxicokinetic Safety Margins

Employing a population based approach, plotting the population frequency distribution of AUC in a histogram, the AUC that would be attained in the different populations through expected consumer use can be visualized in relation to the general adult population AUC that would be achieved at the POD. The comparison can be quantified in a conservative manner by calculating multiples of the AUC between the minimum AUC in the population representing the POD with the maximum AUC in the different populations (figure 14) and could be said to represent a ‘toxicokinetic safety margin’.

Figure 15 shows the simulated AUC distribution of 1000 adult individuals when dosed at HED representing the POD and the simulated AUC in the human populations following either an acute or a chronic consumer dose to show the toxicokinetic safety margin for each population. Full details can be found in Section 4.5 of Burt (2017).

Using this approach negates the need for toxicokinetic extrapolation factors as these are accounted for by using the interspecies differences identified to establish the HED. Intraspecies variability is clearly shown as well as the apparent ‘safety margin’.

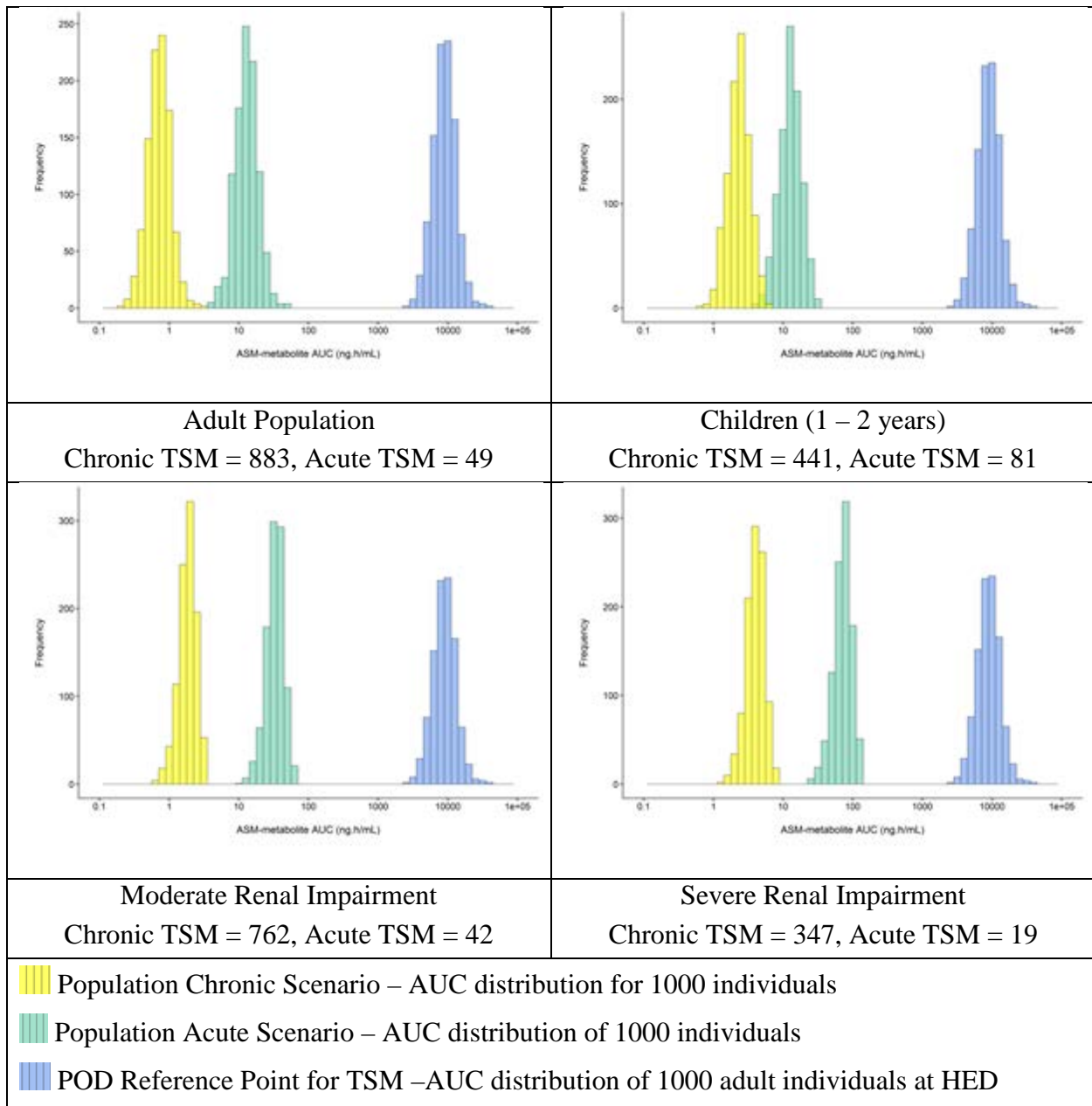


Figure 15: Visualization showing the simulated AUC distribution of 1000 adult individuals when dosed at HED representing the POD and the simulated AUC in the human populations following either an acute or a chronic consumer dose to show the toxicokinetic safety margin for each population.

18 Conclusion

In this proof of concept study we have demonstrated the power of IVIVE and limited rat studies to substantially improve the science underlying the use of uncertainty factors.

Implementing such an approach would reduce uncertainty in risk assessments and move forward towards the goal of maximizing the use of available data and improve the overall scientific basis of a human health risk assessment.

By incorporating population based toxicokinetics and employing a parallelogram approach to aid understanding and subsequent building and verification of IVIVE-PBPK models we have demonstrated how toxicokinetic data derived extrapolation factors can be obtained that not only address interspecies differences but also intraspecies differences within the human population that can be incorporated into conventional human risk assessments.

The population based approach employed allows potentially at risk populations to be identified and examined from a toxicokinetic perspective to quantify a 'toxicokinetic safety margin', expressed in terms of multiples of AUC from the POD, which is maintained when being exposed (dosed) via different consumer exposure scenarios. Utilizing the toxicokinetic safety margin could also form the basis of a human risk assessment based upon internal dosimetry rather than 'external' dose or exposure.

19 References

Burt HJ, Neuhoff S, Lu G, Barter ZE, Jamei M, and Rostami-Hodjegan A (2012) A comparison of single species allometric methods for the prediction of renal clearance in man. *Poster presented at the Simcyp Consortium meeting 2012 (Sheffield, UK)* (provided as PDF to SAP).

Burt H. (2017). Quantitative prediction of the human exposure to acibenzolar-S-methyl and its metabolite. Report number TK0253172 (provided confidentially to SAP).

Chen YT, Trzoss L, Yang D and Yan B (2015) Ontogenic expression of human carboxylesterase-2 and cytochrome P450 3A4 in liver and duodenum: postnatal surge and organ-dependent regulation. *Toxicology* 330:55-61.

<http://www.sciencedirect.com/science/article/pii/S0300483X15000438>

Creton, S., R. Billington, et al. (2009). "Application of toxicokinetics to improve chemical risk assessment: implications for the use of animals." *Regul Toxicol Pharmacol* 55(3): 291-299.

<http://www.sciencedirect.com/science/article/pii/S0273230009001597>

Creton, S., S. A. Saghir, et al. (2012). "Use of toxicokinetics to support chemical evaluation: Informing high dose selection and study interpretation." *Regul Toxicol Pharmacol* 62(2): 241-247. <http://www.sciencedirect.com/science/article/pii/S0273230011002558>

Frost K. (2017). Study to Investigate the In Vitro Absorption, Distribution and Metabolism of Acibenzolar-S-Methyl (CSAA232020) and its Carboxylic Acid Metabolite (CSAA197129). Syngenta Report Number TK0123340 (provided confidentially to SAP).

Howgate EM, Rowland Yeo K, Proctor NJ, Tucker GT and Rostami-Hodjegan A (2006) Prediction of in vivo drug clearance from in vitro data. I: impact of inter-individual variability. *Xenobiotica; the fate of foreign compounds in biological systems* 36:473-497 (provided as PDF to SAP).

Jamei M (2016) Recent Advances in Development and Application of Physiologically-Based Pharmacokinetic (PBPK) Models: a Transition from Academic Curiosity to Regulatory Acceptance. *Curr Pharmacol Rep* 2:161-169 (provided as PDF to SAP).

Jamei M, Marciniak S, Edwards D, Wragg K, Feng K, Barnett A and Rostami-Hodjegan A (2013) The simcyp population based simulator: architecture, implementation, and quality assurance. *In Silico Pharmacol* 1:9 (provided as PDF to SAP).

Jamei M, Marciniak S, Feng K, Barnett A, Tucker G and Rostami-Hodjegan A (2009) The Simcyp population-based ADME simulator. *Expert Opin Drug Metab Toxicol* 5:211-223 (provided as PDF to SAP).

Johnson TN and Rostami-Hodjegan A (2011) Resurgence in the use of physiologically based pharmacokinetic models in pediatric clinical pharmacology: parallel shift in incorporating the

knowledge of biological elements and increased applicability to drug development and clinical practice. *Paediatr Anaesth* 21:291-301 (provided as PDF to SAP).

Jones H and Rowland-Yeo K (2013) Basic concepts in physiologically based pharmacokinetic modeling in drug discovery and development. *CPT Pharmacometrics Syst Pharmacol* 2:e63 (provided as PDF to SAP).

McCoy, A. T., M. J. Bartels, et al. (2012). "TK Modeler version 1.0, a Microsoft(R) Excel(R)-based modeling software for the prediction of diurnal blood/plasma concentration for toxicokinetic use." *Regul Toxicol Pharmacol* 63(2): 333-343.
<http://www.sciencedirect.com/science/article/pii/S0273230012000669>

Molitor E. (1995). Absorption, Distribution, Degradation and Excretion of [U-¹⁴C]Phenyl CGA 245704 in the Rat. Syngenta Report Number 7/95, US EPA MRID 44014250.

Ochodnický P, Henning RH, Buikema H, Kluppel AC, van Wattum M, de Zeeuw D and van Dokkum RP (2009) Renal endothelial function and blood flow predict the individual susceptibility to adriamycin-induced renal damage. *Nephrol Dial Transplant* 24:413-420.
<https://academic.oup.com/ndt/article/24/2/413/1839043/Renal-endothelial-function-and-blood-flow-predict>

Pinto P (2002). CGA-245704 (Acibenzolar-S-Methyl): Developmental Neurotoxicity Study in Rats. Syngenta Report Number 2752-01, US EPA MRID 46046401.

PMRA (2010). PRD 2010-19: Proposed Registration Decision Acibenzolar-S-Methyl,. Health Canada Pest Management Regulatory Agency, Ottawa (provided as PDF to SAP).

Punler M and Tomlinson J. (2017). Acibenzolar-S-methyl: Pharmacokinetics of Acibenzolar-S-methyl and CSAA197129 in the Female Rat Following Single Intravenous Infusion and Oral Administration. Syngenta Report Number 37880 (provided confidentially to SAP).

Rodgers T and Rowland M (2007) Mechanistic approaches to volume of distribution predictions: understanding the processes. *Pharm Res* 24:918-933.
<http://rd.springer.com/article/10.1007/s11095-006-9210-3>

Rostami-Hodjegan A (2012) Physiologically based pharmacokinetics joined with in vitro-in vivo extrapolation of ADME: a marriage under the arch of systems pharmacology. *Clin Pharmacol Ther* 92:50-61 (provided as PDF to SAP).

Rostami-Hodjegan A and Tucker GT (2007) Simulation and prediction of in vivo drug metabolism in human populations from in vitro data. *Nat Rev Drug Discov* 6:140-148 (provided as PDF to SAP).

Rowland Yeo K, Jamei M, Yang J, Tucker GT and Rostami-Hodjegan A (2010) Physiologically based mechanistic modelling to predict complex drug-drug interactions involving simultaneous

competitive and time-dependent enzyme inhibition by parent compound and its metabolite in both liver and gut - the effect of diltiazem on the time-course of exposure to triazolam. *Eur J Pharm Sci* 39:298-309 (provided as PDF to SAP).

Rowland Yeo, K., M. Aarabi, et al. (2011). "Modeling and predicting drug pharmacokinetics in patients with renal impairment." *Expert Rev Clin Pharmacol* 4(2): 261-274 (provided as PDF to SAP).

Sagelsdorff P and Buser G. (1994). CGA-245704 - Investigation of the hydrolytic stability in rat plasma and human serum and tissue homogenates. Syngenta Report Number CB94/20 US EPA MRID 49585201.

Salem F, Johnson TN, Barter ZE, Leeder JS and Rostami-Hodjegan A (2013) Age related changes in fractional elimination pathways for drugs: assessing the impact of variable ontogeny on metabolic drug-drug interactions. *J Clin Pharmacol* 53:857-865 (provided as PDF to SAP).

Sawada Y, Hanano M, Sugiyama Y, Harashima H, and Iga T (1984) Prediction of the volumes of distribution of basic drugs in humans based on data from animals. *J Pharmacokinetic Biopharm* 12:587-596. <http://rd.springer.com/article/10.1007/BF01059554>

Shi D, Yang D, Prinssen EP, Davies BE and Yan B (2011) Surge in expression of carboxylesterase 1 during the post-neonatal stage enables a rapid gain of the capacity to activate the anti-influenza prodrug oseltamivir. *The Journal of infectious diseases* 203:937-942. <https://academic.oup.com/jid/article/203/7/937/1036019/Surge-in-Expression-of-Carboxylesterase-1-During>

Turner D, Musther H, Jamei M, and Rostami-Hodjegan A (2011) A mechanistic model for the prediction of human equilibrium blood-to-plasma concentration ratio (B/P): basic and neutral drugs. *Poster presented at the AAPS annual meeting 2011 (Washington DC, USA)* (provided as PDF to SAP)

US EPA (2009a). Acibenzolar-S-Methyl – Revised Acute and Chronic Dietary and Drinking Water Exposure and Risk Assessments. Office of Prevention, Pesticides and Toxic Substances. Washington.

US EPA (2009b). Revised Acibenzolar-S-methyl Human Health Risk Assessment for Proposed Use of Acibenzolar-S-methyl on Cucurbits and Bulb Onions. Office of Prevention, Pesticides and Toxic Substances. Washington.

US EPA (2012). Acibenzolar-S-methyl Establishment of Temporary Tolerances on Experimental Use Permit Request. Office of Chemical Safety and Pollution Prevention. Washington.

US EPA (2014). Guidance for Applying Quantitative Data to Develop Data-Derived Extrapolation Factors for Interspecies and Intraspecies Extrapolation Office of the Science Advisor Risk Assessment Forum. Washington

World Health Organization/International Program on Chemical Safety (WHO/ IPCS), (2005) Chemical-specific adjustment factors for interspecies differences and human variability: Guidance document for use of data in dose/concentration–response assessment. International Program on Chemical Safety, WHO/UNEP/ILO, Geneva, Switzerland.

Yang D, Pearce RE, Wang X, Gaedigk R, Wan YJ and Yan B (2009) Human carboxylesterases HCE1 and HCE2: ontogenic expression, inter-individual variability and differential hydrolysis of oseltamivir, aspirin, deltamethrin and permethrin. *Biochem Pharmacol* 77:238-247.
<http://www.sciencedirect.com/science/article/pii/S0006295208007168>

Yuan, J. (1993). "Modeling blood/plasma concentrations in dosed feed and dosed drinking water toxicology studies." *Toxicol Appl Pharmacol* 119(1): 131-141.
<http://www.sciencedirect.com/science/article/pii/S0041008X83710525>

Zhu HJ, Appel DI, Jiang Y and Markowitz JS (2009) Age- and sex-related expression and activity of carboxylesterase 1 and 2 in mouse and human liver. *Drug Metab Dispos* 37:1819-1825. <http://dmd.aspetjournals.org/content/37/9/1819.short>

Appendix 1: Toxicology Endpoints and Point of Departure

Acibenzolar has been evaluated in acute and repeat dose toxicity studies in rats, mice, rabbits and dogs, and in developmental toxicity studies in rats and rabbits, and reproductive toxicity and developmental neurotoxicity studies in rats (US EPA 2009; PMRA 2010; US EPA 2012).

Acibenzolar has low acute toxicity, is non-irritating to rabbit eyes and skin, and was a skin sensitizer in the guinea pig. Signs of toxicity were similar in rats, mice and dogs and included decreased body weight, body weight gain, mild regenerative anemia, and changes in the spleen. Repeat dose studies relevant to the determination of toxicity endpoints are outlined in Table A1.

Table A1: Repeat Dose Toxicity Studies Relevant to Toxicity Endpoint Determination

Study, Route & Species	Dose levels	NO(A)EL	LOAEL	Effects
28-day gavage Tif rat	10, 100, 800 mg/kg	100 mg/kg NOEL	800 mg/kg	Decreased body weight, body weight gain, food consumption and food efficiency both sexes. Decreased RBC and WBC parameters altered clinical chemistry parameters, decreased thymus weight, increased hemosiderosis in the absence of extramedullary haematopoiesis in the spleen, and necrotic hepatocytes, effects more predominant in females.
90-day dietary Tif rat	40, 400, 2000, 8000 ppm M : 0, 2.42, 24.6, 126, 516 mg/kg F: 0, 2.64, 26.3, 131, 554 mg/kg	126/131 mg/kg	516/554 mg/kg	Decreased body weight, reduced food intake and efficiency and increased liver and spleen weights
2-year dietary Tif rat	20, 200, 2500, 7500 ppm M: 0.77, 7.77, 96.9, 312 mg/kg F: 0.90, 9.08, 111, 388 mg/kg	96.9/111 mg/kg	312/388	Decreased body weights, body weight gain and food efficiency, mild hemolytic anemia, and increased incidence of alveolar foam cells (females only).
Prenatal developmental toxicity gavage Tif rat	10, 50, 200, 400 mg/kg	Maternal 200 mg/kg Developmental 50 mg/kg	Maternal 400 mg/kg Developmental 200 mg/kg	Maternal: reduced maternal body weight development and hemorrhagic perineal discharge Developmental: increased incidence skeletal variations
Prenatal developmental toxicity CD rat	10, 75, 150, 350 mg/kg	Maternal 350 mg/kg Developmental 150 mg/kg	Maternal > 350 mg/kg Developmental 350 mg/kg	Developmental: increased incidence lumbar rib

Two generation reproduction dietary Tif rat	20, 200, 2000, 4000 ppm	Parental 200 ppm Reproductive 4000 ppm Developmental 200 ppm	Parental 2000 ppm Reproductive > 4000 ppm Developmental 2000 ppm	Parental: increased spleen weight and hemosiderosis Developmental: decreased pup weight and pup weight gain
Developmental neurotoxicity dietary Wistar-derived rat	100, 1000, 4000 ppm 8.2, 82, 326 mg/kg	Maternal 326 mg/kg Developmental Neurotoxicity 326 mg/kg	Maternal > 326 mg/kg Developmental Neurotoxicity > 326 mg/kg	Developmental Neurotoxicity: Small changes in brain morphometry in males at 82 and 326 mg/kg were considered not of toxicological significance
90-day dietary dog	0, 10, 50 , 200 mg/kg	50 mg/kg	200 mg/kg	Decreased body weight gain, increased liver weight, regenerative anemia, splenic erythropoiesis
1-year dog	0, 5, 25, 200	25 mg/kg	200 mg/kg	Increased liver weight, anemia, hemosiderosis, splenic erythropoiesis

The lowest potential point of departure (POD) in the acibenzolar data base is 8.2 mg/kg/day taken from the developmental neurotoxicity study. This point of departure has been used by the US EPA (US EPA 2009a; US EPA 2012), as the basis for acute reference doses (ARfD) for all populations, for the chronic reference dose (CRfD) for females ages 13 to 49 and for young children of 0.082 mg/kg, while 25 mg/kg is the basis for the CRfD for men and women over 49 (US EPA 2012). Health Canada PMRA (PMRA 2010) uses 8.2 mg/kg for both acute and chronic dietary risk assessments for all populations.

To be conservative and consistent with existing regulatory opinion, 8.2 mg/kg/day is used as the POD for the purposes of demonstrating the utility of our approach.

Appendix 2: PBPK Model Input, Output and R Script Files Provided to the SAP

Files have been provided containing all Simcyp workspaces, Simcyp outputs, R script and output from R analysis relating to the PBPK modelling of Acibenzolar and its metabolite, acibenzolar-acid, as reported in Burt, 2017. The files are numbered according to the section in which they can be found in the report.

The generic file types are as follows:

.wksz	Model input (workspace) files (these can only be viewed within the Simcyp simulator)
.xlsx	Full model output files (see table below for details)

In order to perform additional analysis, the acibenzolar-acid concentrations were extracted from the original output files (.xlsx) and further analyzed in R. The additional analysis performed by the R script provides the following information:

- The clearance of acibenzolar-acid (on the assumption of complete conversion from acibenzolar)
- For the chronic dosing scenario, the exposure (AUC) for the final dosing interval (24 hours) of chronic dosing

The R scripts for each simulation are denoted as **.R** files and the resulting **.csv** files are labelled as follows:

out_ind_params.csv	Acibenzolar-acid PK parameters for each simulated individual
out_pop_params.csv	Summary of acibenzolar-acid PK parameters for the entire population
out_profile.csv	Acibenzolar-acid concentration-time profile for each individual
out_profile_summary.csv	Summary of acibenzolar-acid concentration-time profile for the population (mean, 5th and 95th percentiles)
raw concentration data.csv	The raw data extracted from the Excel simulation outputs (.xlsx). R reads the data from the csv file and then calculates the PK parameters.

Additional files for specific simulations have also been provided and are detailed below:

Section 4.1.1 Rat IV dosing

Only input files (.wksz) and the full output (.xlsx) have been provided.

Section 4.1.2 Rat oral dosing

Only input files (.wksz) and the full output (.xlsx) have been provided for 1, 10 and 100 mg/kg as this was prior to the introduction of variability into the rat model.

Additional files for metabolite administration at 10 mg/kg only (input .wksz and output .xlsx) are provided to demonstrate that due to rapid and complete conversion of acibenzolar to acibenzolar acid during first pass, the PK of acibenzolar-acid could be simulated by direct infusion into blood at a rate equal to the acibenzolar absorption rate (with dose corrected for metabolite).

Section 4.1.3 Rat oral dosing with simulated variability

Input (.wksz) and full output files (.xlsx) are provided for simulations in rat at 1, 10, 100 mg/kg incorporating variability.

To incorporate variability, the simulations were performed in Simcyp via an R script to:

- Load the initial Simcyp workspace (.wksx)
- Generate virtual individuals with variability around specified parameters
- Run a simulation in each individual
- Collate results into .csv files as described above

The R script for introduction of variability (.R) is provided.

The same set of files is provided for simulations at 10 mg/kg without variability in renal clearance included.

Section 4.2 Simulation of acibenzolar-acid concentrations in the rat DNT study

The input file (.wksz) used for all simulations relating to the rat DNT study is provided.

Section 4.2.1 Dose input file during the rat DNT study

The R script (.R) used to determine the overall absorption rate for each 2 hour period of the day, based on the rate of consumption and rate of absorption is provided (.R) along with the results (.csv). From these the amount absorbed in each 2 hour period was calculated.

Section 4.2.2 Simulated acibenzolar-acid exposure during the rat DNT study

The files provided are as described above for section 4.1.3 for dosing at 8.2 mg/kg/day.

Section 4.3 Simulation of the human pharmacokinetics of acibenzolar and its metabolite after acute and chronic oral dosing

In each of the human populations, two scenarios were simulated following acute and chronic exposure. Pediatric simulations were performed both at the pediatric dose and at the adult dose.

For each population and dosing scenario, the input (.wksz), full output (.xlsx), R script (.R) and results (.csv) files are provided as described above.

Section 4.3.6 Dose proportionality and determination of a human equivalent dose

Files are provided for the simulation of acibenzolar and acibenzolar-acid exposure following administration of the human equivalent dose.

For both acibenzolar and acibenzolar-acid, the input (.wksz), full output (.xlsx), R script (.R) and results (.csv) files are provided as described above.

Section 4.4 and 4.5 Calculation of exposure margins

An excel file is provided detailing the calculation of the exposure margins between human consumer exposure and either the exposure at the simulated rat POD dose or the human equivalent dose.

The calculations were performed from the **out_pop_params.csv** files generated in section 4.2.2 (Rat DNT study) and section 4.3.6 (HED for acibenzolar-acid) and the human populations described in section 4.3.

Section 4.6 Sensitivity of simulated acibenzolar and acibenzolar-acid concentrations to parameter uncertainty

Excel files containing the results of the sensitivity analysis on plasma half-life, renal clearance, blood-to-plasma ratio and absorption rate constant are provided.

The following worksheets are present in the full excel output files (.xlsx):

Worksheet	Description
Summary	Overview of the model setup, including the dose metrics simulated
Input Sheets:	
Input Sheet	Main listing of parameters for the model
Ode State Info	State variables
Sim-population	Parameters for the population being simulated. Worksheet name will change with the population.
Demographic Data	Physiological parameters for each individual simulated
Drug-Population Parameters	Compound specific parameters for each individual simulated
Enzymatic Status Esterase	Metabolic parameters for each individual simulated
Output Sheets:	
Clearance Trials SS	Clearance by individual at steady state
Substrate Clearance Values	Clearance by individual by substrate
% fm and fe SS	Metabolism and excretion by individual
Absorption	Absorption by individual
Conc Trials Profiles(CBlood)	Mean Values of Systemic concentration in blood of acibenzolar considering the effects of its metabolite over Time
Sub Pri Met1(Trials)(CBlood)	Mean Values of Systemic concentration in blood of acibenzolar-acid
Conc Profiles CSys(CBlood)	Mean Values of Systemic concentration in blood of Acibenzolar over Time
Sub Pri Met1(CBlood)	Mean Values of Systemic concentration in blood of acibenzolar-acid
CLint profiles	Parent clearance rates by process
CLint Profiles (Pri Met1)	Metabolite clearance rates by process
AUC0(Sub)(CBlood)	Parent blood AUCs by individual
AUC0(Sub PM1)(CBlood)	Metabolite blood AUCs by individual
Distribution - Vols	Volumes of distribution by individual
Distribution - Kps	Partition coefficients by individual